ลักษณะภาพรังสีส่วนตัดอาศัยคอมพิวเตอร์ของต่อมน้ำเหลืองภายในทรวงอกของแมวปกติ

นางสาวนิลวรรณ ธรรมศิริ

วิทยานิพนธ์นี้เป็นส่วนหนึ่งของการศึกษาตามหลักสูตรปริญญาวิทยาศาสตรมหาบัณฑิต
สาขาวิชาศัลยศาสตร์ทางสัตวแพทย์ ภาควิชาศัลยศาสตร์
คณะสัตวแพทยศาสตร์ จุฬาลงกรณ์มหาวิทยาลัย
ปีการศึกษา 2560

COMPUTED TOMOGRAPHY APPEARANCE OF INTRA-THORACIC LYMPH NODES IN NORMAL CATS

Miss Ninlawan Thammasiri

A Thesis Submitted in Partial Fulfillment of the Requirements
for the Degree of Master of Science Program in Veterinary Surgery
Department of Veterinary Surgery
Faculty of Veterinary Science
Chulalongkorn University
Academic Year 2017

Thesis Title	COMPUTED TOMOGRAPHY APPEARANCE OF INTRA-THORACIC LYMPH NODES IN NORMAL CATS
By	Miss Ninlawan Thammasiri
Field of Study	Veterinary Surgery
Thesis Advisor	Assistant Professor Nan Choisunirachon, D.V.M., M.Sc., Ph.D., D.T.B.V.S.
Thesis Co-Advisor	Assistant Professor Damri Darawiroj, D.V.M., M.Sc., Ph.D.

Accepted by the Faculty of Veterinary Science, Chulalongkorn University in Partial Fulfillment of the Requirements for the Master's Degree

.....Dean of the Faculty of Veterinary Science
(Professor Roongroje Thanawongnuwech, D.V.M., M.S., Ph.D., D.T.B.V.P.)

THESIS COMMITTEE

.....Chairman
(Assistant Professor Kumpanart Soontornvipart, D.V.M., Ph.D., D.T.B.V.S.)

.....Thesis Advisor
(Assistant Professor Nan Choisunirachon, D.V.M., M.Sc., Ph.D., D.T.B.V.S.)

.....Thesis Co-Advisor
(Assistant Professor Damri Darawiroj, D.V.M., M.Sc., Ph.D.)

.....Examiner
(Panrawee Phoomvuthisarn, D.V.M., M.Sc., Ph.D.)

.....External Examiner
(Assistant Professor Tassanee Jaroensong, D.V.M., Ph.D., D.T.B.V.M.)

นิลวรรณ ธรรมศิริ : ลักษณะภาพรังสีส่วนตัดอาศัยคอมพิวเตอร์ของต่อมน้ำเหลืองภายในทรวงอกของแมวปกติ (COMPUTED TOMOGRAPHY APPEARANCE OF INTRA-THORACIC LYMPH NODES IN NORMAL CATS) อ.ที่ปรึกษาวิทยานิพนธ์หลัก: ผศ. สพญ. ดร.แนน ช้อยสุนิรชร, อ.ที่ปรึกษาวิทยานิพนธ์ร่วม: ผศ. นสพ. ดร.ดำริ ดาราวิโรจน์, 79 หน้า.

การศึกษาลักษณะของต่อมน้ำเหลืองภายในทรวงอกของแมวบนภาพรังสีส่วนตัดอาศัยคอมพิวเตอร์ โดยทำการศึกษาในซากแมวเสียชีวิต แมวมีชีวิตที่มีลักษณะทางคลินิกปกติ และการศึกษาย้อนหลังจากประวัติแมวป่วยที่เข้ารับการตรวจวินิจฉัยด้วยการถ่ายภาพรังสีส่วนตัดอาศัยคอมพิวเตอร์ จากผลการศึกษาพบว่า ไม่สามารถตรวจพบต่อมน้ำเหลืองภายในทรวงอกของซากแมวบนภาพรังสีส่วนตัดอาศัยคอมพิวเตอร์ ทว่าเมื่อศึกษาในแมวมีชีวิตที่มีลักษณะปกติทางคลินิกจำนวน 30 ราย คละสายพันธุ์ อายุระหว่าง 4 เดือน ถึง 11 ปี น้ำหนักตัวระหว่าง 1.5 ถึง 5.7 กิโลกรัม แมวเพศผู้จำนวน 12 ตัว (ทำหมันจำนวน 6 ตัว) และ แมวเพศเมียจำนวน 18 ตัว (ทำหมันจำนวน 10 ตัว) คะแนนความสมบูรณ์ของร่างกายมีค่าระหว่าง 2 ถึง 5 พบว่าในแมวเด็กที่มีอายุต่ำกว่า 7 เดือน สามารถตรวจพบต่อมน้ำเหลืองได้น้อยกว่าแมวที่มีอายุมากกว่า 7 เดือน นอกจากนั้น ในแมวปกติสามารถตรวจพบต่อมน้ำเหลืองได้เฉพาะบริเวณกระดูกสันอก (6/30) ประจันอก (10/30) และทางแยกหลอดลม (7/30) บนภาพรังสีส่วนตัดอาศัยคอมพิวเตอร์ภายหลังการฉีดสารเพิ่มความชัดภาพ แต่ตรวจไม่พบต่อมน้ำเลืองบริเวณกระดูกซี่โครง (0/30) ความกว้างของต่อมน้ำเหลืองบริเวณกระดูกสันอก ประจันอก และทางแยกหลอดลมบนภาพด้านตัดขวางของภาพรังสีส่วนตัดอาศัยคอมพิวเตอร์ภายหลังการฉีดสารเพิ่มความชัดภาพ มีค่าเท่ากับ 4.18 ± 1.62 มิลลิเมตร 5.70 ± 2.41 มิลลิเมตร และ 4.30 ± 2.19 มิลลิเมตรตามลำดับ เมื่อเปรียบเทียบการตั้งค่าการบันทึกภาพรังสีส่วนตัดอาศัยคอมพิวเตอร์พบว่าความหนาภาพที่1.25มิลลิเมตร ให้คะแนนการตรวจพบต่อมน้ำเหลืองในทรวงอกของแมวปกติไม่แตกต่างจากความหนาภาพที่0.625 มิลลิเมตร ($p > 0.05$). สำหรับการศึกษาย้อนหลังจากประวัติสัตว์ป่วยแมวเข้าร่วมในการศึกษาจำนวน 9 ตัว ไม่พบปุ่มน้ำเหลืองในทรวงอกของแมวบนภาพรังสีส่วนตัดอาศัยคอมพิวเตอร์ในแมวจำนวน 8 ตัว และตรวจพบก้อนเนื้อบริเวณประจันอกในแมวจำนวน 1 ตัว

ภาควิชา	ศัลยศาสตร์	ลายมือชื่อนิสิต .....
สาขาวิชา	ศัลยศาสตร์ทางสัตวแพทย์	ลายมือชื่อ อ.ที่ปรึกษาหลัก .....
ปีการศึกษา	2560	ลายมือชื่อ อ.ที่ปรึกษาร่วม .....

5875312331 : MAJOR VETERINARY SURGERY
KEYWORDS: CAT / COMPUTED TOMOGRAPHY / LYMPH NODES / NORMAL / THORACIC

NINLAWAN THAMMASIRI: COMPUTED TOMOGRAPHY APPEARANCE OF INTRA-THORACIC LYMPH NODES IN NORMAL CATS. ADVISOR: ASST. PROF. NAN CHOISUNIRACHON, D.V.M., M.Sc., Ph.D., D.T.B.V.S., CO-ADVISOR: ASST. PROF. DAMRI DARAWIROJ, D.V.M., M.Sc., Ph.D., 79 pp.

The study of the appearance of intra-thoracic lymph nodes in the cat observed on the computed tomography which divided into 3 parts as following; the feline soft cadaver, clinically normal cats and the retrospective study of the feline patients. The result showed that the computed tomographic images of feline soft tissue cadavers could not detected any intra-thoracic lymph nodes. However, based on the study on 30 clinically normal cats which were mixed breed, age ranging from 4 months to 11 years old, body weight between 1.5 to 5.7 kilogram, 12 male cats (6 castrated) and 18 female cats (10 spayed) and body condition score between 2 to 5, intra-thoracic lymph nodes could be more detected in the cat that the age was more than 7 months old. Besides, only the sternal, cranial mediastinal and tracheobronchial lymph nodes could be detected on the post-contrast enhanced CT images, but not the intercostal lymph node (6/30, 10/30, 7/30 and 0/30 nodes, respectively). The maximal wideness of the sternal, cranial mediastinal and tracheobronchial lymph node on the axial, post-contrast enhanced CT images were 4.18 ± 1.62 mm, 5.70 ± 2.41 mm and 4.30 ± 2.19 mm, respectively. Comparing between the CT machine setting, the slice thickness at the 1.25 mm showed the similar detection score of the normal intra-thoracic lymph node as that of the 0.625 mm ($p > 0.05$). Finally, based on the retrospective study, 9 cats were included. The intra-thoracic lymph nodes of 8 cats could not be detected, but a cat revealed a large cranial mediastinal mass.

Department:	Veterinary Surgery	Student's Signature	.....
Field of Study:	Veterinary Surgery	Advisor's Signature	.....
Academic Year:	2017	Co-Advisor's Signature	.....

ACKNOWLEDGEMENTS

I would like to express my deepest thankful to my dearest thesis advisor, Asst. Prof. Dr. Nan Choisunirachon, for her greatest dedication, invaluable advisement, sincerest and warmest encouragement throughout many years. I am truly appreciated her devotion, patience and kindness from all my heart. Furthermore, I am also sincerely thanks my thesis co-advisor, Asst. Prof. Dr. Damri Darawiroj, for his kindness in precious advisement and writing format proofing.

I am heartedly appreciated to all my thesis committee (Assist. Prof. Dr. Kumpanart Soontornvipart, Assist. Prof. Dr. Tassanee Charoensong and Dr. Panrawee Phoomvuthisarn) for their great helpful and insightful comments to fulfill my thesis.

I am wholeheartedly thanks you to Miss Aomusa Kuaha, Miss Chutimon Thanaboonnipat, Miss Urapa Klansnoh, all clinician, staffs of The Diagnostic Imaging Unit, The Small Animal Teaching Hospital, as well as my graduated colleague, Department of Veterinary Surgery, Faculty of Veterinary Science, Chulalongkorn University, and other persons whom I have not been mentioned for their assistance, friendship and encouragement.

Finally, I would like to express my heartfelt and overwhelming gratitude to my dearest parents and family, for their advisement, caring, endless love, understanding and everlasting support throughout my whole life. Without them, I would not be accomplished my graduation after all.

CONTENTS

Page

Page

Page

LIST OF FIGURES

LIST OF TABLES

LIST OF ABBREVIATIONS

ALB	=	albumin
ALP	=	alkaline phosphatase
ALT	=	alanine aminotransferase
BUN	=	blood urea nitrogen
CRT	=	capillary refill time
CT	=	Computed Tomography
DSH	=	domestic short hair
FeLV	=	Feline Leukemia Virus
FIV	=	Feline Immunodeficiency Virus
FOV	=	field of view
HU	=	Hounsfiled Unit
H	=	height
HR	=	heart rate
Kg	=	kilograms
L	=	length
mm.	=	millimeter
mm^3	=	square millimeter
MM	=	mucous membrane
3D MPR	=	3 Dimensional Multiplanar Reconstruction
mgI/BW	=	milligram iodine per body weight
MHz	=	megahertz
RR	=	respiratory rate
R^2	=	coefficient of determine
r	=	correlation coefficient
SD	=	standard deviation

TP	=	total protein
U/S	=	Ultrasonography
W	=	width
WL	=	Window Level
WW	=	Window Width

CHAPTER 1

INTRODUCTION

Importance and Rationale

The lymphatic system is a part of the circulatory system and acts as a defend mechanism to resist any anatomical changes to various local or systemic inflammatory, infection, or neoplastic stimuli. In the body, the lymphatic system is composed of the circulating lymph, lymphatic vessels and lymphatic organs (Aspinall and O'Reilly, 2004).

Among lymphatic organs, lymph node is a soft tissue organ that internal parenchyma is composed of lymphoid tissue. The normal location of lymph node is located along the lymphatic vessels and the node could be detected only at the superficial area by palpation. During the pathologic conditions such as inflammation, viral infection or malignant tumors, lymphadenopathy, the condition of the lymph node that increase in size and change in shape, contour and texture, could be detected (Rogers et al., 1993). Clinically diagnostic evaluation of lymph node usually performs by physical examination to detect the appearances, size, shape, and consistency, only the superficial area can achieve though. Furthermore, diagnostic imaging methods by survey radiography, lymphangiography, ultrasonography, or computed tomography (CT), and invasive laboratory methods by means of fine needle aspiration for cytologic examination or tissue biopsy for histopathology provide more information of the affected lymph node.

In cats, there are several symptoms or diseases caused lymphadenopathy at the deep anatomical areas both at intra-thoracic and intra-abdominal cavities. For example, Feline Immunodeficiency Virus (FIV) that cause the generalized lymphadenopathy during the first stage after viral infection (Magden et al., 2011), Feline

Leukemia Virus (FeLV) that induced abdominal lymphadenopathy and alimentary lymphoma that could cause mesenteric lymphadenopathy (Ettinger, 2003; Louwerens et al., 2005). Hugo and Heading (2015) reported that Feline Coronavirus, the cause of Feline Infectious Peritonitis (FIP), could induce lymphadenopathy both of intra-thoracic and intra-abdominal lymph nodes. To observe the intra-thoracic lymph node, especially mild to moderate alteration, diagnostic imaging is usually hard to accomplish. According to the limitation of intra-thoracic ultrasonography due to the gas accumulation in lung parenchyma and less sensitivity of thoracic radiographs to detect the early lymphadenopathy, advanced diagnostic imaging likes CT that provides transverse anatomical images would be beneficial to assess the intra-thoracic lymph node status.

To evaluate lymph nodes, there are several factors need to be concerned. It has been reported that the appearance of intra-cavity, normal lymph nodes was interfered by surrounded fat accumulation (Beukers et al., 2013). Moreover, other factors such as age could influence to the size of lymph nodes. Nemanic and Nelson (2012) revealed that juvenile animals have larger lymph node size than that of the maturation based on ultrasonograms and CT images. Nowadays, there has no published information of intra-thoracic lymph nodes, all of appearance, shape, size and architectural patterns both of before and after contrast enhanced-CT images in cats. Therefore, this research was aimed to investigate the appearance including other factors that could effect to the normal intra-thoracic lymph nodes in cats. The results of this study might be beneficial for using as the reference value on clinical diagnostic imaging in small animal practice.

Objectives of study

- To investigate the gross anatomy and computed tomographic appearance of intra-thoracic lymph nodes in feline soft cadavers.
- To evaluate the appearance of normal intra-thoracic lymph nodes at each area both of before and after contrast enhanced-CT scan.
- To evaluate the factor such as sex, age, body weight and body condition score of the cat affected to appearance of normal intra-thoracic lymph nodes.
- To evaluate the parameter of CT machine such as slice thickness on the feasibility to detect the location of intra-thoracic lymph nodes at each area both of before and after contrast enhanced-CT scan.

Key word (Thai) :

แมว, ภาพถ่ายรังสีส่วนตัดอาศัยคอมพิวเตอร์, ต่อมน้ำเหลือง, ปกติ, ทรวงอก

Key word (English) :

Cat, Computed tomography, Lymph nodes, Normal, Thoracic

Hypothesis

1. In healthy cat, the normal appearance of intra-thoracic lymph nodes should be similar in appearance, position, shape and architextural pattern both of before- and after-contrast enhanced-CT.
2. Age, sex, body weight and body condition score could effect to the appearance of normal lymph nodes in thoracic cavity.
3. Slice thickness at different level such as 0.625 mm, 1.25 mm, 2.5 mm, and 5 mm of both before- and after-contrast enhanced-CT could effect on the feasibility to identify of intra-thoracic lymph nodes in each area.

CHAPTER 2

LITERATURE REVIEW

The lymphatic system

The lymphatic system is a part of the defense mechanism in mammalian body, which composed of circulating lymph, lymphatic vessel and lymphatic organs (Figure 1). There are several functions of the lymphatic system (Aspinall and O'Reilly, 2004), which include

- Returning of excess extracellular fluid, which is called lymph, to the circulatory system.
- Carrying on products composing of fat digestion, fat-soluble vitamins from gastrointestinal tract to the circulation.
- Producing lymphocyte that is an important part of immune system in the mammalian body.
- Eliminating of antigen foreign body or migrated tumor cells in the lymph to lymph nodes.

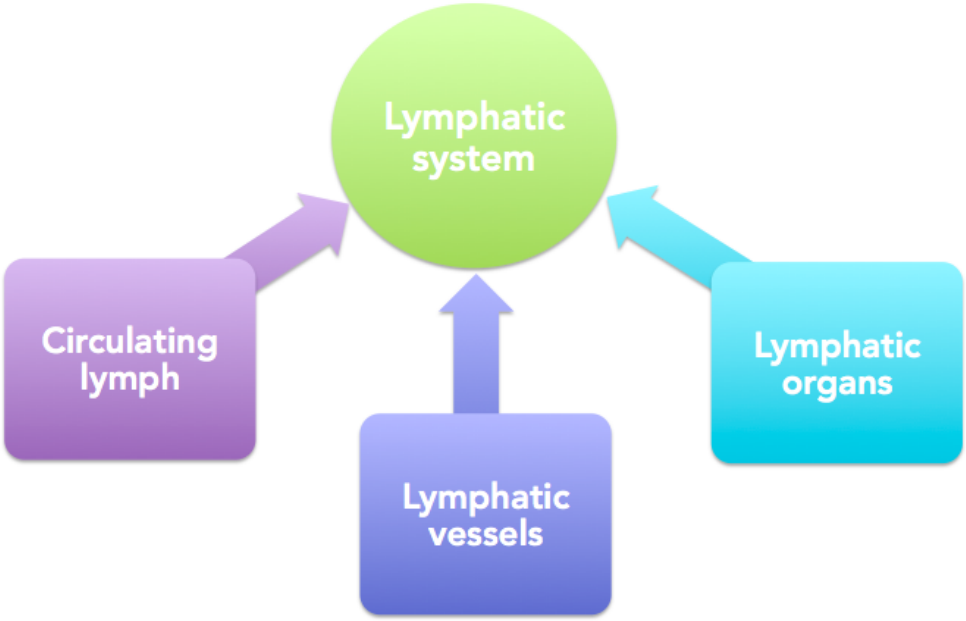

Figure 1 *The structure of lymphatic system.*

Although, there are different in anatomical structures among lymph, lymphatic vessel and lymphatic organs especially the lymph nodes, their functions are related. Before returning to the circulation, lymph and carrying substances are transported through the lymph vessel and intermittently pass through the lymph node that focally located along the lymphatic vessels. Lymph node is kidney bean-shaped which inside contains lymphoid tissue. Lymph node is covered by thin capsule that there is an indented area calling hilus (Aspinall and O'Reilly, 2004). The hilar area is composed of efferent lymphatic vessel, artery and vein. In contrast to efferent lymphatic vessel, which is the exit of lymph from the lymph node, lymph entrances into lymph node through the multiportal afferent lymphatic vessels at the convex side (Aspinall and O'Reilly, 2004; Little, 2012). Internally, each node is supported by network fibrous connective tissue called trabecular (Figure 2). Microscopically, lymph node is divided into two compartments; the outer parenchyma called cortex and inner parenchyma

named medulla. The cortex of lymph node is composed of follicles of B cells that enclosed by T cells whereas medullary area contains tissue macrophages, lymphocyte, and plasma cell. The area between the cortex and medulla, which comprises antigen-presenting cell originally from small T cells and macrophages, is called the paracortical area (Little, 2012). Due to the location and internal structure, lymph nodes act as the mechanical filters for interstitial fluid or lymph that may contains or carries microorganisms, particles or migrated tumor cells.

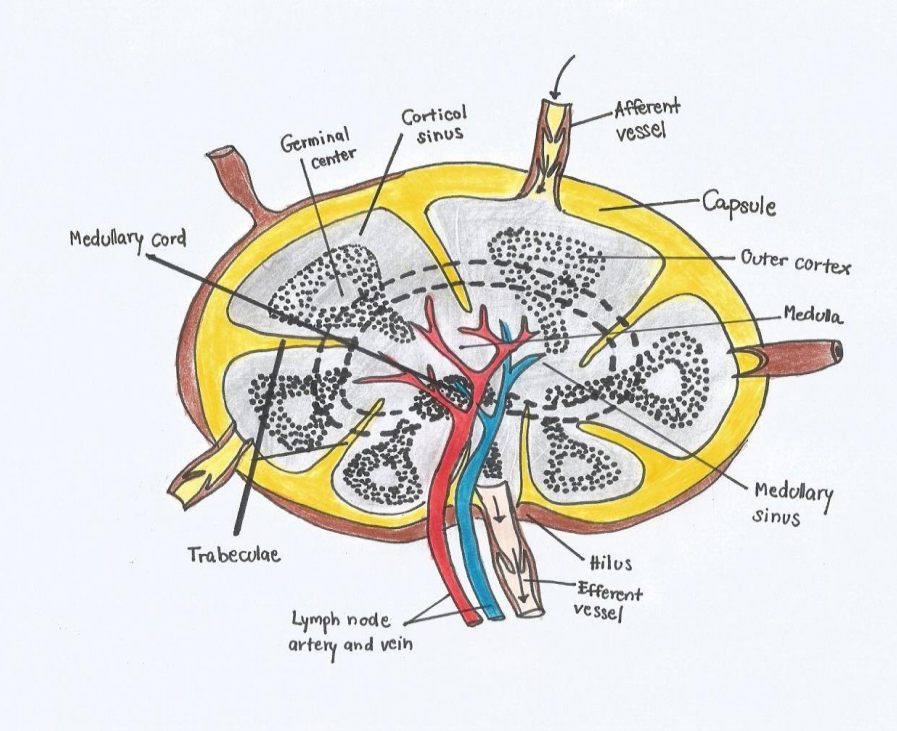

Figure 2 *The internal structure of lymph node.*

During pathological processes, adjacent lymph nodes respond by increase in size, change in shape and firm in consistency, which is called “lymphadenopathy”(Rogers et al., 1993). In cat, there are several conditions or diseases causing lymphadenopathy such as infectious diseases, e.g. bacterial, fungal, or viral infection, non-infectious diseases e.g. idiopathic condition or hyperplasia, inflammation, and neoplastic or non-neoplastic condition (Figure 3). Lymphadenopathy may happen as single location called solitary lymphadenopathy, or generalized affectation found as multiple lymphadenopathy. Etiologies causing lymphadenopathy of cat, both of solitary and generalized lymphadenopathy, are shown in Table 1 (Little, 2012).

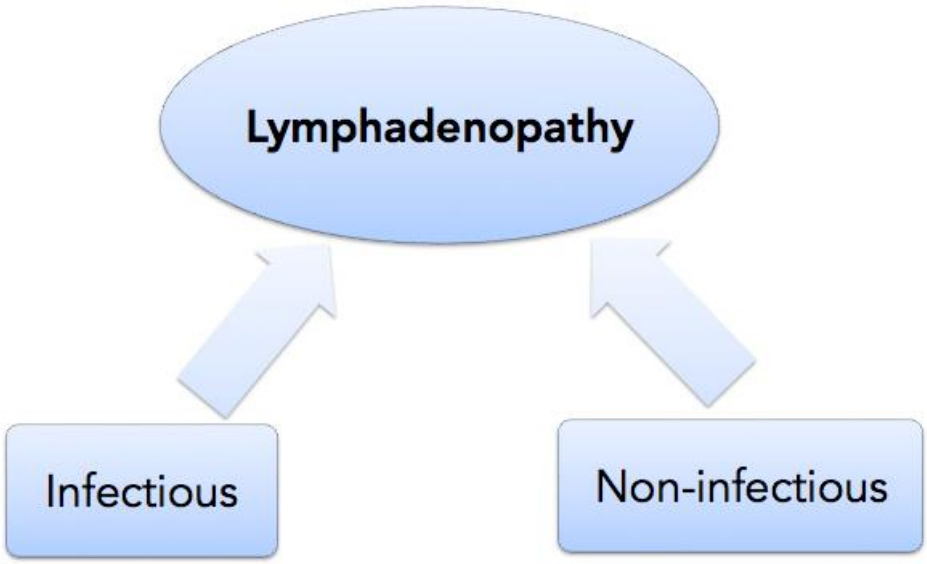

Figure 3 *Cause of lymphadenopathy.*

Table 1 *Etiology causing lymphadenopathy (Little, 2012).*

Solitary lymphadenopathy	Generalized lymphadenopathy
- Infectious	**- Infectious**
Bacteria:	*Bacteria:*
- Mycobacteriosis	
- Hemoplasmosis	
- Various other organisms	
Fungus:	
- Histioplasmosis	
- Blastomycosis	
- Cryptococcosis	
- Sporotrichosis	
- Phycomycosis	
Virus:	*Virus:*
- Feline leukemia virus	- Feline leukemia virus
- Feline immunodeficiency virus	- Feline immunodeficiency virus
- Feline infectious peritonitis	- Feline infectious peritonitis
	- Post-vaccination
- Noninfectious	**- Noninfectious**
	Immune mediated:
	- Chronic progressive polyarthritis
Idiopathic:	*Idiopathic:*
- Plexiform vascularization	- Distinctive lymph nodes hyperplasia of young cats
- Distinctive lymph node hyperplasia of young cats	- Generalized lymphadenopathy resembling lymphosarcoma

Local inflammation	
Neoplasia:	*Neoplasia:*
- Hemolymphatic neoplasms	- Lymphosarcoma
- Metastatic neoplasia	- Myelolymphoproliferative disease
	- Myeloma
	- Mast cell tumor
Non-neoplasia:	*Non-neoplasia:*
- Eosinophilic granuloma complex	- Hypereosinophilic syndrome

The diagnostic evaluation of lymph nodes in cats is generally performed by physical examination to detect size, shape and consistency. However, only the superficial lymph nodes could be successfully achieved. Other techniques that could be applied and provide more information of lymph nodes are survey radiograph, lymphangiography, ultrasonography, including cytologic or histologic examinations through fine needle aspiration or tissue biopsy, which latter is an invasive technique (Rogers et al., 1993). In cats, there are several conditions or diseases that may cause intra-cavity lymphadenopathy, especially at intra-thoracic cavity. For example; infectious diseases by viral infection such as FIV (Louwerens et al., 2005; Seo et al., 2006; Magden et al., 2011) and feline corona virus (Hugo and Heading, 2015), or parasitic infection by *Aelurostrongylus abstrusus* (Dennler et al., 2013; Lacava et al., 2016). Furthermore, Vanstennkiste and colleagues (2014) reported that grass seed foreign bodies in thoracic cavity in cats are also caused intra-thoracic lymphadenopathy. In addition, due to the better quality of life of companion animals, there are an increasing number of geriatric cats presented to the small animal practitioner. Among aging diseases, neoplasia is one of the abnormalities that need to be closely supervised. According to that the malignant tumor is prone to migrate to distant organs, the most

frequent method performing to check the tumor staging is intra-thoracic screening for both of pulmonary nodules and intra-thoracic lymphadenopathy (Beukers et al., 2013). According to the former information and conventional diagnostic imaging methods are hard to evaluated the small size of intra-thoracic lymph nodes due to the less sensitivity of radiograph (Figure. 4 and 5) and the gas artifact of non-cardiac ultrasonography (Figure. 6), advanced imaging diagnostic methods such as computed tomography (CT) (Figure. 7) that displays the volumetric data of anatomical structures will be a superior diagnostic tool.

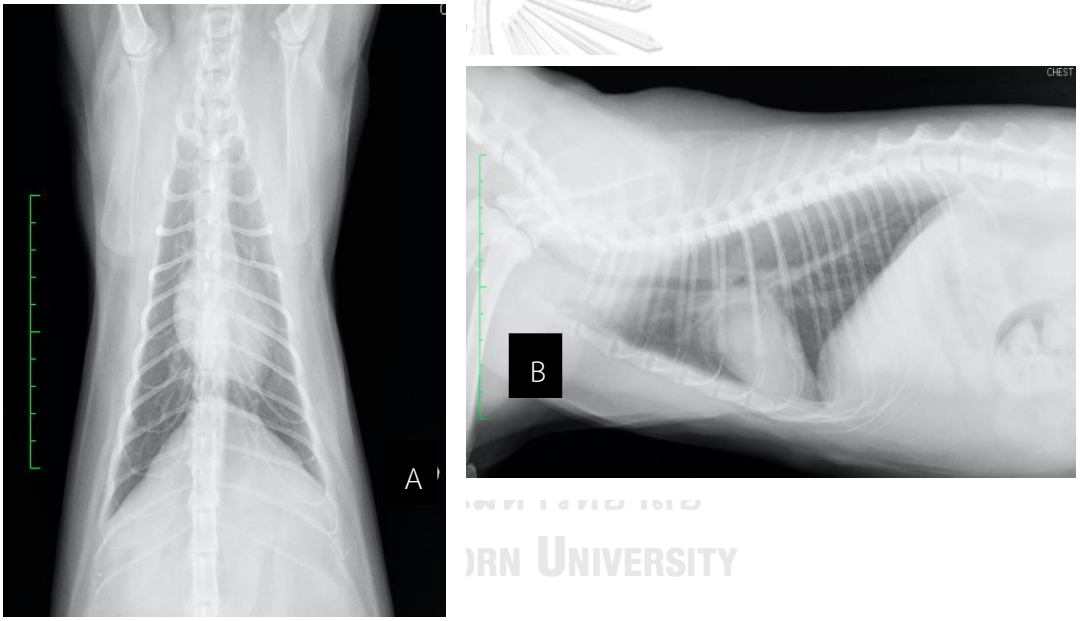

Figure 4 *Thoracic radiographs of normal cat both of (A) ventrodorsal (B) lateral views.*

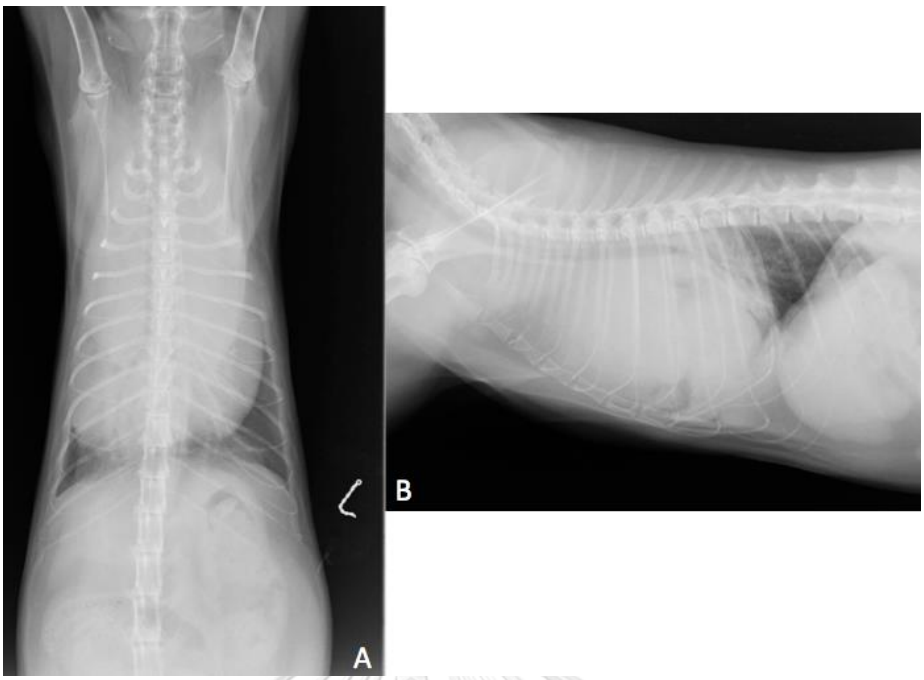

Figure 5 *Thoracic radiographs, both of ventrodorsal (A) and lateral views (B) of a cat with lymphoma induced cranial mediastinal mass.*

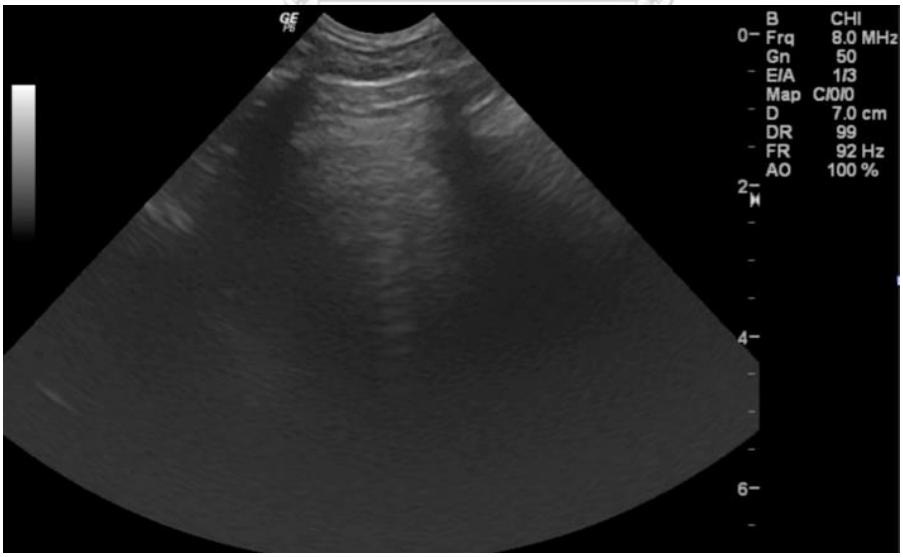

Figure 6 *Thoracic ultrasonography.*

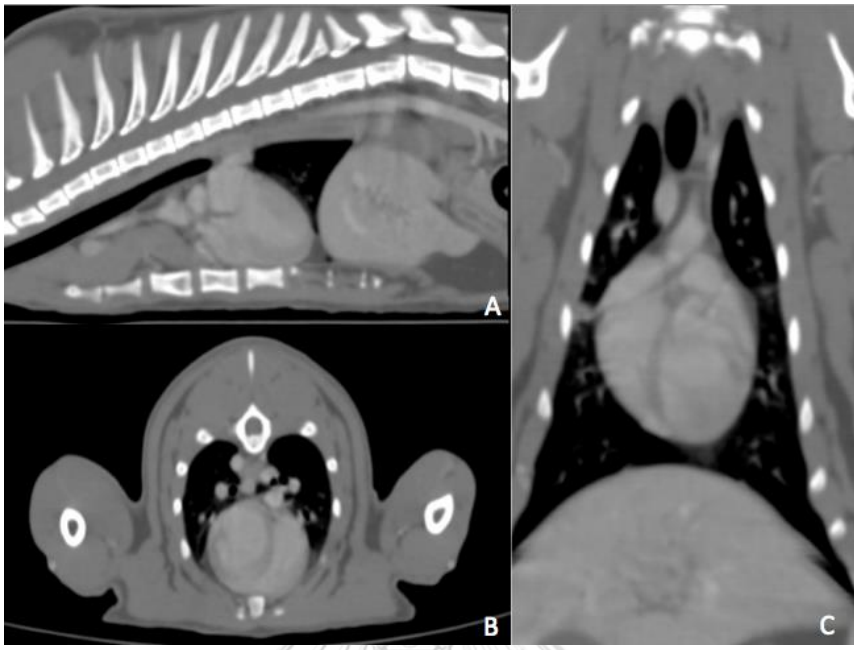

Figure 7 *Thoracic computed tomography all of (A) sagittal (B) transverse (C) Coronal planes.*

In veterinary medicine, CT has been applied for neurological, oncological and orthopedic diseases, both in canine and feline patients (Ohlerth and Scharf, 2007; Bertolini and Prokop, 2011). After the axial or helical X radiation to the patient, the rest of non-absorbed X-ray will be computerized recorded and displayed on the gray scale image. In addition to the computerized processing of CT images that provide multiplanar reconstruction (MPR) for anatomical structure (Figure 8), the gray scale images, measured as the Hounsfield Unit (HU), could be multilevel displayed (Figure 9). To achieve that, there are two factors that controlling the grey scale, which are window width (WW) and window level (WL) (Ohlerth and Scharf, 2007). Therefore, both of multiplanar reconstruction and multi-window settings of CT (Table 2) will distinctively exhibit the suspected organ, especially the small structure such as lymph node.

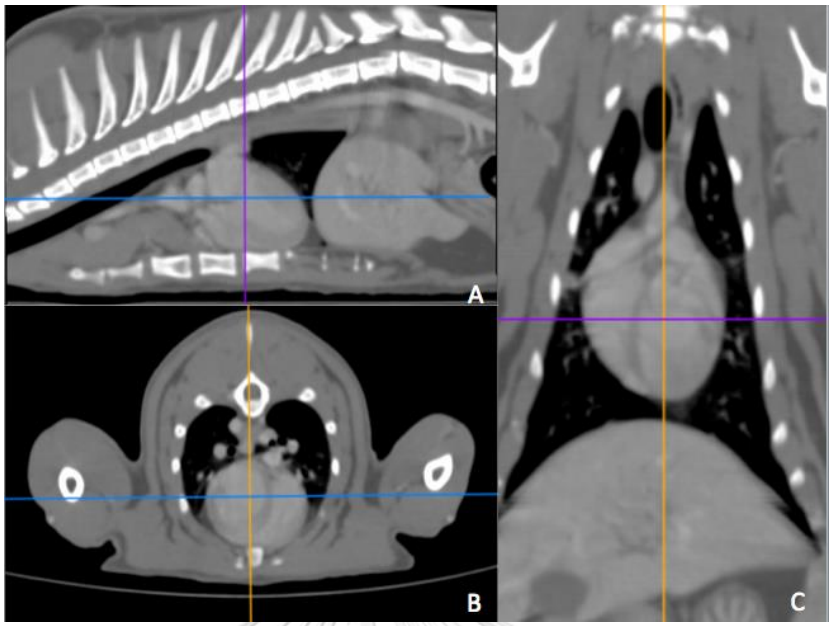

Figure 8 *3D Multiplanar reconstruction (3D MPR) of thoracic CT images on each plane such as sagittal (A), axial (B) and coronal planes (C).*

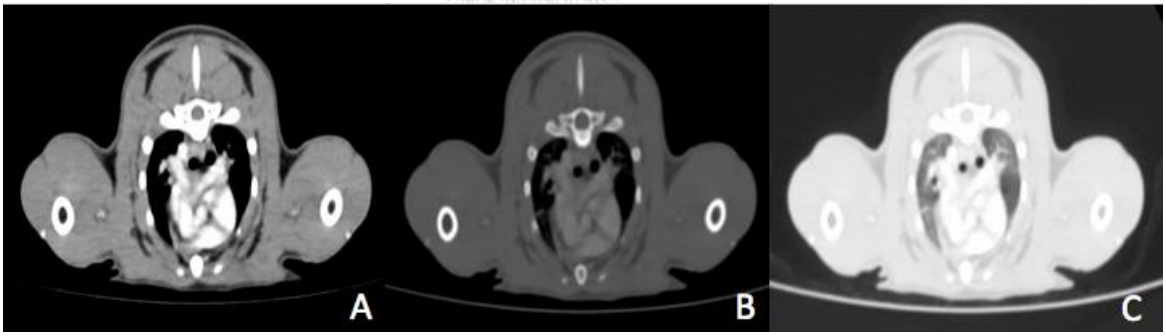

Figure 9 Gray scale levels of CT thoracic images. Note that (A) Soft tissue (B) Bone (C) Pulmonary.

Table 2 Suggestions of different window settings for the application of CT in small animals (W = window width; WL = window level; HU = Hounsfield Unit) (Ohlerth and Scharf, 2007).

Window	**WW (HU)**	**WL (HU)**
Bone	400-500	>1500
Soft tissue	40-50	500-400
Brain	35	150
Pituitary gland	80	250
Mediastinum	50-	400
Lung	500-	1500

During imaging diagnosis, there are several factors need to be concerned prior differentiating the lymphadenopathy from the normal lymph node. It has been reported that juvenile animal has larger lymph node size than that of the grown up animal (Nemanic and Nelson, 2012). Besides, normal lymph nodes in some areas are often disabling to detect based on imaging diagnosis. Nemanic and Nelson (2012) reported that the intra-cavity fat accumulation around the lymph node was one of factor that effect to the lymph node detection. According to the previous information and there has no published data for the facts of intra-thoracic lymph nodes based on CT images in normal cats, the purposes of this study was to investigate the appearance of normal intra-thoracic lymph node including other information such as shape, size, architextural pattern both of before- and after-contrast enhancement. Furthermore, the factors such as age, sex, body, and weight and body condition score of the cats that may effect to the appearance of normal lymph node were explored. The result from this study would be useful as a reference value on clinical diagnostic imaging in small animal clinical practice.

CHAPTER 3

MATERIALS AND METHODS

Animals

The animal that has been used in this study was divided into 3 groups in according to the study parts, which were

Part 1: The gross appearance and computed tomographic appearance of intra-thoracic lymph nodes in presumed normal thorax of feline soft tissue cadavers.

Three feline soft cadavers that their histories were died due to the causes without intra-thoracic related diseases. The general information such as signalment and preview history were noted.

Part 2: The CT appearance of intra-thoracic lymph node in normal cat.

This study was approved by The Institutional Animal Care and Use Committee of Chulalongkorn University (CU-IACUC), the approval number: 1631073. Thirty, client-owned, clinical healthy cats were recruited in this study and divided into three groups of different ages, which were as the following information:

Group 1: Juvenile cats, age younger than 7 months old.

Group 2: Mature cats, age between 7 months to 7 years old.

Group 3: Senile cats, age older than 7 years old.

Prior the computed tomographic study, all signalment of the enrolled cats such as breed, age, sex including the neutered status, body weight and body condition score were noted. Furthermore, all cats were physically and laboratory screened to confirm to be normal status by means of physical examination, hematology, serum biochemistry, urinalysis, serologic examination of endemic viral diseases such as Feline Immunodeficiency Virus (FIV) and Feline Leukemia Virus (FeLV), and basic diagnostic imaging both of radiography and ultrasonography.

Physical examination

All cats were evaluated for general appearance, mentation, hydration status, temperature, heart rate (HR) and rhythm, respiratory rate (RR) and character, mucous membrane color (MM), capillary refill time (CRT), palpated peripheral lymph nodes, abdominal palpation.

Hematology and serum biochemistry

Complete blood count, blood chemistry includes blood urea nitrogen (BUN), creatinine (CRE), alkaline phosphatase (ALP), alanine aminotransferase (ALT), total protein (TP) and albumin (ALB) were checked in all cats.

Urinalysis

Urinalysis in all cats was performed to check the appearance, concentration and content of urine by strip test (Combur-Test® strip, Roche, Cobas, Switzerland) and microscopic finding.

Serologic examination for FeLV and FIV

Serologic examination for *FeLV* and *FIV* was done by using of the in-house serologic test kit (Witness®, Zoetis, Lyon, France). Cats with positive result of test kit were excluded from this study.

Basic diagnostic imaging

According to some maladies, especially infectious diseases, could cause generalized lymphadenopathy, all cats were screened and confirmed that do not affected by any diseases causing the lymphadenopathy by thoracic radiography and abdominal radiography including abdominal ultrasonography.

Thoracic and abdominal radiographic procedures

Thoracic and abdominal radiography were performed in ventrodorsal and lateral views. Thoracic radiography was taken to cover the whole area of the thoracic cavity ranging from thoracic inlet to the caudal area of the 13^{th} thoracic vertebral column. For abdominal radiography, the field of view (FOV) was designed to cover the area from the cranial of diaphragm to the mid pelvic canal.

Abdominal ultrasonographic procedure

Abdominal ultrasonography was done to examine for all of abdominal organs. Ultrasonography was performed with linear transducer operating at 7.0 MHz. Each cat was positioned in dorsal recumbency in V-shaped pad. The hair over the region of interest at the ventral abdomen was clipped and skin was cleaned with 70% alcohol. Prior the examination, acoustic coupling gel was applied to allow the sound transmission and linear transducer was used to capture the ultrasonogram. All abdominal organs include liver; gall bladder, spleen, adrenal glands, kidneys, urinary bladder, gastrointestinal tract, and pancreas were examined. Cats that revealed one of the abnormalities from the screening procedures, the cat would be excluded from the study.

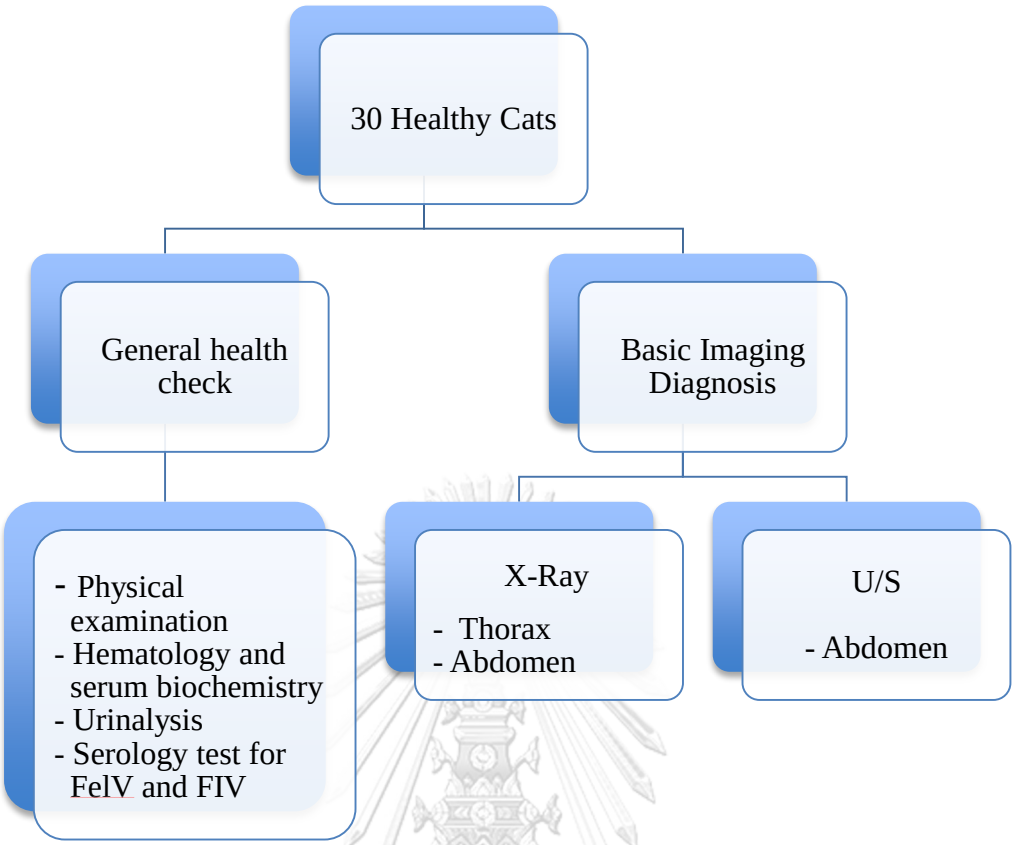

Figure 10 *Conceptual framework of diagnostic screening methods for enrolled cats prior the computer tomographic investigation.*

Part 3: The CT appearance of intra-thoracic lymph node in feline patients.

CT data of feline patient that has been performed the CT scan as the diagnostic method at The Diagnostic Imaging Unit, The Small Animal Teaching Hospital, Faculty of Veterinary Science, Chulalongkorn University during May 2013 to March 2017 were retrieved. The inclusion criteria were the CT data of feline patient that the FOV was covered the thoracic cage and both of pre- and post-contrasts enhancement phases were available. All information such as signalment, physical examination, laboratory examination including the CT appearance such as size, shape, contour and architextural pattern of the intra-thoracic lymph nodes both of before and after contrast enhancement and final diagnosis information were noted and compared.

CT scan procedures

Due to the anesthetic procedure during the CT examination, all alive cats were withheld from food and drink at least 8 and 6 hours, respectively, for preventing of aspiration pneumonia. Prior the sedation, all cats were physical examined to check mucous membrane color, dehydration status, body temperature, body condition score, body weight, heart rate, respiratory rate. Then, disposable intravenous catheter was inserted into the cephalic vein at the anti-brachium of the right forelimb. Subsequently, the intravenous crystalloid fluid (Acetar®) was parentally administrated at the rate of 5 - 10 ml per kgBW. All cats were sedated by acepromazine maleate (Combistress®, Antwerp, Belgium) dose 0.03 mg/kg and tramadol hydrochloride (Tramache®, Baroda, India) dose 2 mg/kgBW intramuscularly, and the general anesthesia was induced by propofol (Lipuro®1%, Melsungen, Germany) dose 2 - 4 mg/kg BW intravenously. Cats were then intubulated with disposable endotracheal tube and are maintained the general anesthesia with isofurane (Isofurane®, Bethlehem, U.S.A.) at the concentration of 2 - 5% in pure oxygen. Each cat, both alive and soft tissue cadavers were then positioned in sternal recumbency with the direction of the head is pointed to the CT gantry and thoracic cavity is perpendicular to the isocenter of CT scan planes (Figure 11 and 12).

Figure 11 *Computed tomography machine.*

Figure 12 *Computed tomography of enrolled cat. The head of the cat was pointed to the CT gantry.*

Before the CT images (both of pre- and post-contrast enhancements) were obtained, the pre-scan or scout phase that X-ray was radiated to produce 2 directional, perpendicular radiographs of the cat was performed by using a 64-slice, helical CT unit with peak kilovoltage of 120 kVp and amperage of 10 mA. The length of the body on the pre-scan images was started from the rostal area of nostril to the caudal region of perineum. To obtain the pre- and post-contrast enhanced CT images, the FOV was created to cover all dimensions of thoracic cage ranging from thoracic inlet to the caudal area of the 13th thoracic vertebral column (Figure 13).

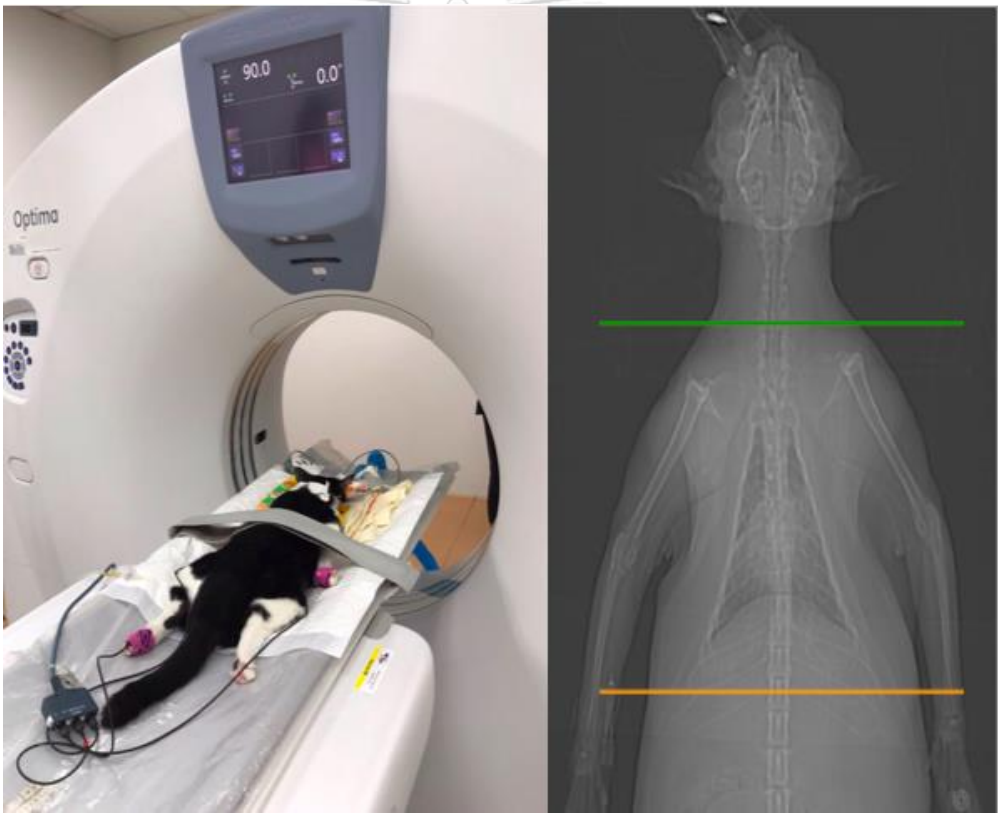

Figure 13 *Computed tomographic positioning and field of view of thoracic CT scan.*

The CT scanning was performed by using the following parameters; a low-pass filter, slice thickness 1.25 mm, collimator pitch 0.969, matrix of 512 x 512, peak kilovoltage of 120 kVp and smart amperage with automate dose reduction. After finishing the pre-contrast enhanced phase, non-ionic, iodine contrast medium using iohexol (Omnipaque 300®, Cork, Ireland) was manually intravenous administrated at the dose of 600 mgI/kgBW in alive cats and the post-contrast enhanced CT images were subsequently achieved at the same FOV of the pre-contrast enhanced phase. CT images from soft tissue cadavers and alive cat (all of pre- and post-contrast enhanced phases) were collected and reconstructed to be various slice thickness as following 0.625, 1.25, 2.5 and 5 mm, and data were saved as the DICOM files (Figure 14).

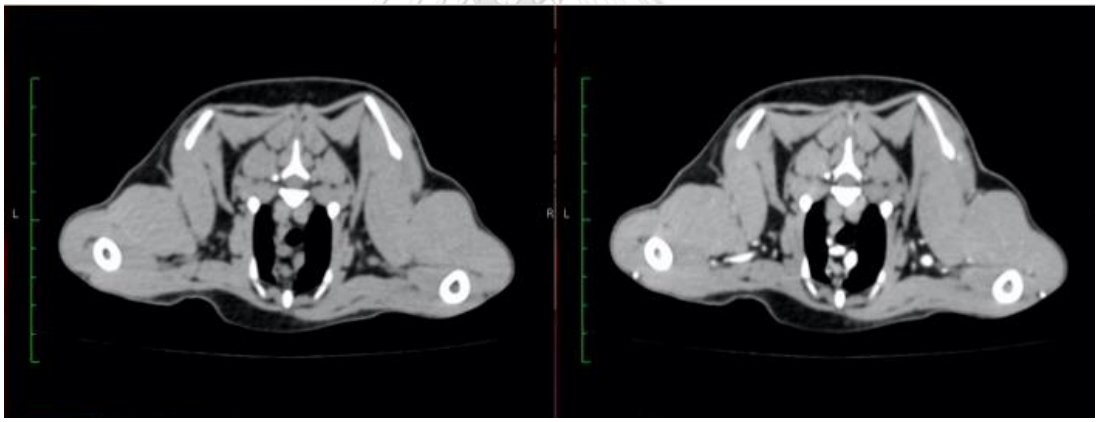

Figure 14 *Pre- and Post - contrast enhancement CT image.*

As soon as the CT scanning procedure was finished, the feline soft cadavers were subjected to the autopsy procedure. After dissection, the information, for example appearance, size, shape and number of intra-thoracic lymph node of each area as following, sternal lymph node, tracheobronchial lymph node, cranial mediastinum lymph node and intercostal lymph node, were recorded (Figure 15 and Table 3).

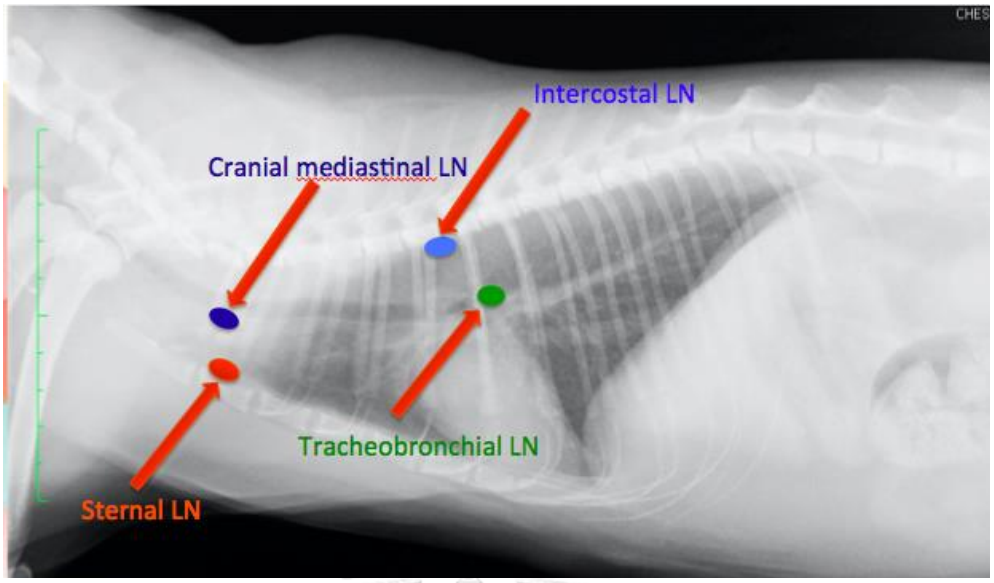

Figure 15 *Normal intra-thoracic lymph nodes.*

Table 3 *Normal intra-thoracic lymph nodes (Dyce et al., 2010).*

Lymph nodes	Location	Function
Sternal lymph node	Embedded in fat beside the sternum at the level of the second rib	Receive lymph from the muscle of the ventral thoracic wall, diaphragm, and the mediastinum and may collaborate with the axillary lymph nodes in draining the first three pairs of mammary glands and their efferent vessels go to veins at thoracic inlet.

Cranial mediastinal lymph node	Variously, related to the large blood vessels in front of the heart	Drain structures in the mediastinum (including the tracheobronchial nodes) and deep muscles at the base of the neck and their outflow also enter the veins at thoracic inlet.
Tracheobronchial lymph node	Scattered around the tracheal bifurcation	Drain the lungs as well as mediastinal structures and part of the diaphragm and their efferent vessels pass to the cranial mediastinal nodes.
Intercostal lymph node	Maybe present under the pleura at the dorsal end of fifth or sixth intercostal space	Drains the structure of the dorsal thoracic wall and sends its efferent vessels to the cranial mediastinal nodes.

Computed tomographic data collection and analysis

CT images were processed by the image viewer using OsiriX® software. Images were analyzed by soft tissue window using 350 HU of WW and 40 HU of WL. Appearance such shape, contour, architextural pattern both of pre- and post – contrast enhancement images in alive cats were recorded for each of the following intra-thoracic lymph nodes (Table 3, Figure 15)

- Sternal lymph node
- Cranial mediastinal lymph nodes
- Tracheobronchial lymph node
- Intercostal lymph node

In addition, MPR was applied for indicating the maximal size in each dimension (Figure16). In addition to the size of intra-thoracic lymph nodes at each dimension, the volume of node was calculated using the ellipsoidal volume by the equation

$$\frac{3}{4}\pi ab^2$$

Besides, the feasibility of detection or detection score for intra-thoracic lymph nodes at the 0.625 mm-reconstructed images were given as

0: lymph node could not be detected.

1: lymph node was probably detected.

2: lymph node could be detected but the appearance was not distinct.

3: lymph node could be detected with distinct appearance.

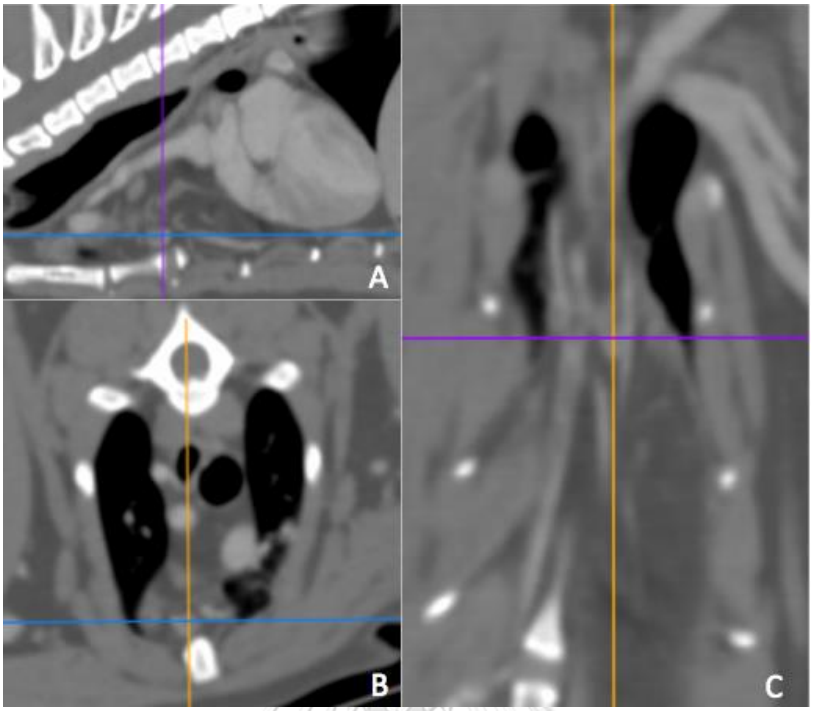

Figure 16 *3D Multiplanar reconstruction (3D MPR) of CT images on sagittal (A), axial (B) and coronal (C) planes to indicate the maximal size of sternal lymph node.*

Furthermore, the detection score as former description will be applied to compare between the intra-thoracic lymph nodes at each area at the different CT slice thickness such as 0.625, 1.25, 2.5, and 5 mm.

The feasibility to detect all of intra-thoracic lymph nodes were also compared to the body weight, body condition score and degree of obesity which the later was calculated from the average lateral thoracic wall fat thickness at the mid thoracic area (carina area) to the thoracic vertebral height on the same image (Figure 21).

$$\text{Degree of obesity} = \frac{\text{average lateral thoracic wall fat thickness at the mid thoracic area (carina area)}}{\text{thoracic vertebral height}}$$

The degree of obesity was divided to three groups of

Group 1: degree of obesity < 1

Group 2: degree of obesity 1 - 2

Group 3: degree of obesity > 2

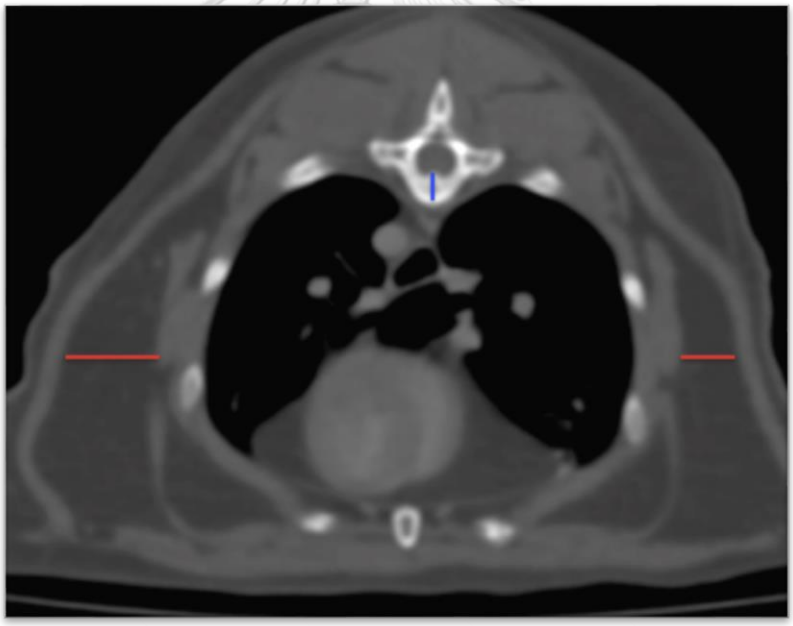

Figure 17 *The axial CT image at the mid thoracic area (carina area) showed the degree of obesity derived by the average lateral thoracic wall fat thickness (red bars) by the thoracic vertebral height (blue bar) on the same image.*

Statistical analysis

All data especially in the part 1 and 3 were described as the descriptive data. The numeric data were reported as the mean including the standard deviation. In addition, to compare the effect of sex on other parameters, unpaired T-test was applied whereas the other effects were observed by Kruskal-Wallis test. The correlation between the body weight including body condition score and degree of obesity was observed by the Pearson correlation test. All statistical analysis was performed using Prism7 (Graphpad software, California, USA). All statistical significance will be considered if $p < 0.05$.

CHAPTER 4

RESULTS

Part 1: The gross appearance and computed tomographic appearance of intra-thoracic lymph nodes in presumed normal thorax of feline soft tissue cadavers.

Clinical features

The clinical features of 3 feline soft cadavers were shown in Table 4. There were 2 males (castrated 1) and 1 spayed female. DSH was the most common breeds (n = 2) and a Persian cat. The mean ± SD of age was 80.00 ± 86.81 months or 6.66 ± 7.23 years. The mean ± SD of body weight was 4.13 ± 1.15 kg. The minimal body condition score was 2 and the maximal body condition score was 4 of 5. The mean ± SD of body condition score was 3.0 ± 1.0.

All feline soft cadavers were died without history of intra-thoracic related disease. After cadavers had investigated by CT scan, CT images at difference slice thickness at 0.625, 1.25, 2.5, and 5.0 mm were recorded only at pre-contrast enhancement for determination of the appearance of all intra-thoracic lymph nodes. After that cadavers were subjected to the autopsy to recorded data of lymph nodes.

The appearance of all intra-thoracic lymph nodes on pre-contrast enhanced CT images could not be detected. However, only one of soft cadavers revealed 3 locations of intra-thoracic lymph nodes on autopsy i.e. sternal, cranial mediastinal and tracheobronchial lymph node.

Sternal lymph nodes was found 1 position of embedded in fat above the second sternebra (Figure 18). The size of sternal lymph node was 3.0 x 6.0 x 1.0 mm (W x L x H). Cranial mediastinal lymph nodes were found at least 2 positions that scattered into the cranial mediastinal fat next to the large blood vessels (Figure 19). The average size of cranial mediastinal lymph node was 3.0 x 4.0 x 1.0 mm (W x L x H). Tracheobronchial lymph nodes were found at least 3 positions that scattered at

the termination of trachea and principal bronchi (Figure 20). The average size of tracheobronchial lymph node was 3.6 x 8.8 x 2.0 mm (W x L x H). Then, all of lymph node which found from autopsy had brought to investigated by histopathology for confirm lymphoid tissue of sample (Figure 21). In addition, the intercostal lymph node was not detected on both of pre-contrast enhanced CT images and autopsy.

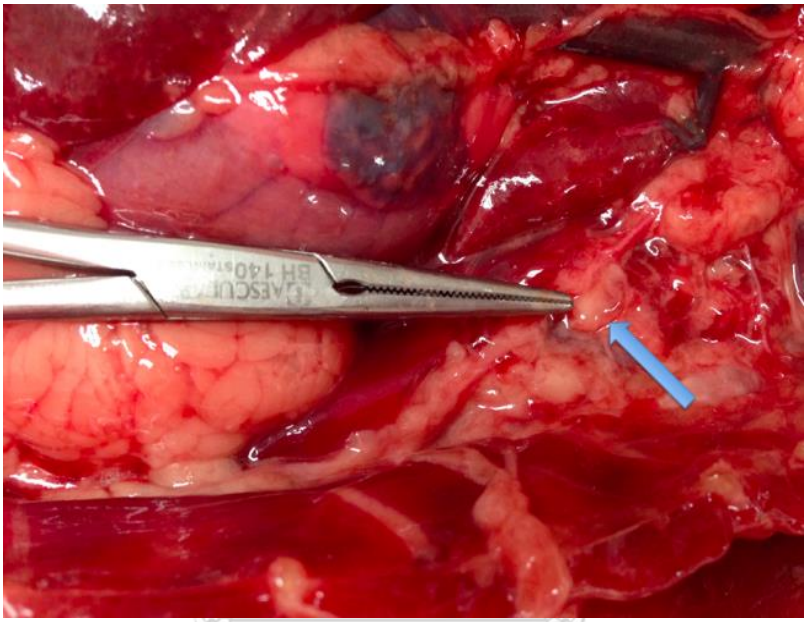

Figure 18 *Sternal lymph node (arrow).*

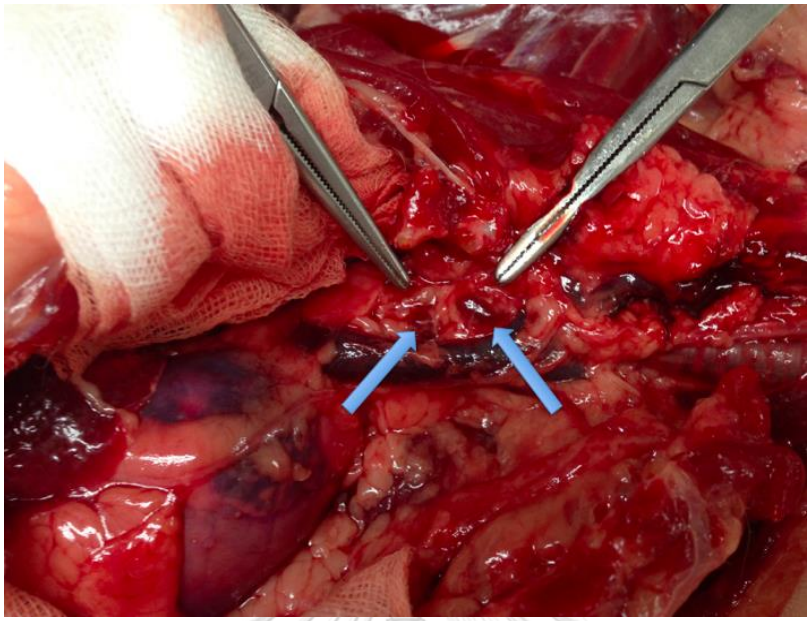

Figure 19 *Cranial mediastinal lymph node (arrows).*

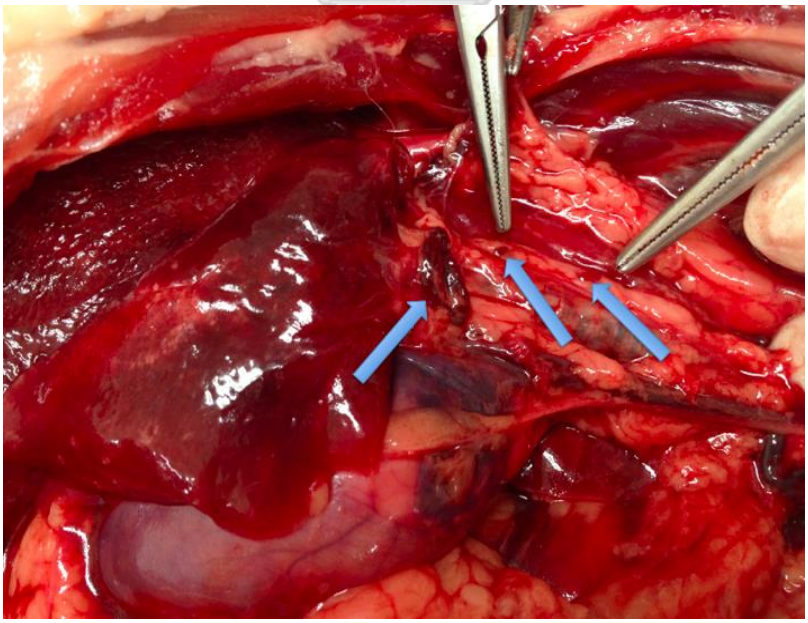

Figure 20 *Tracheobronchial lymph node (arrows).*

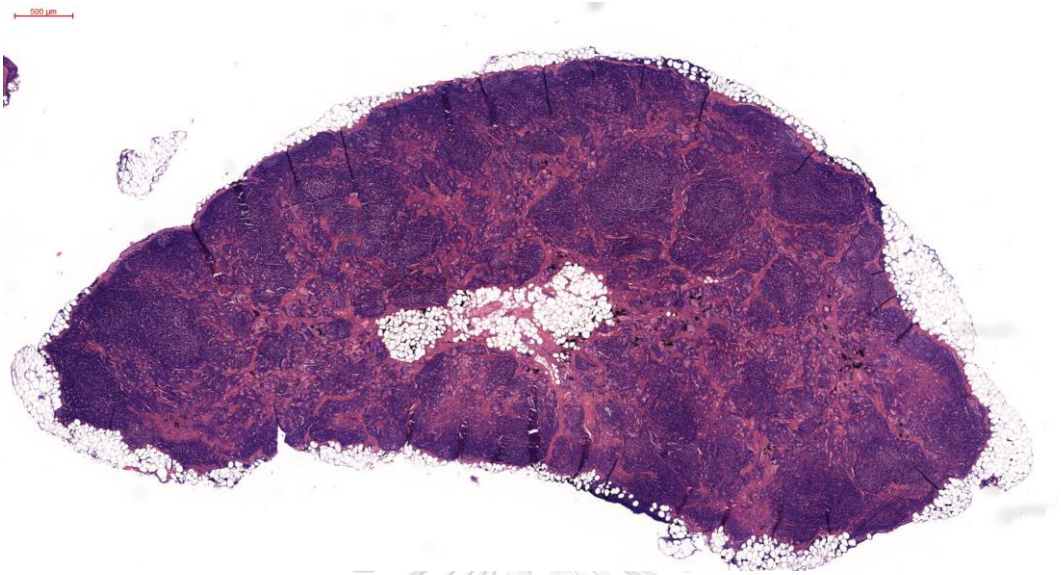

Figure 21 *Histopathological image of intra-thoracic lymph node from feline soft cadaver by autopsy.*

Table 4 *Clinical demographic data of feline soft cadavers.*

Clinical features		Value
No. of cadavers		3
Age (months)		
	Median	80
	Mean ± SD	80.00 ± 86.81
	Range	(24 - 180)
Sex		
	Female	1
	Intact	1
	Spayed	0
	Male	2
	Intact	1
	Castrated	1
Weight (kg.)		
	Median	4.13
	Mean ± SD	4.13 ± 1.15
	Range	(3.0 - 5.3)
Body condition score (5)		
	Median	3
	Mean ± SD	3.0 ± 1.0
	Range	(2 – 4)

Part 2: The CT appearance of intra-thoracic lymph node in normal cats.

Clinical features

The clinical features of the 30 normal cats are shown in Table 5. There were 12 males (castrated 6) and 18 females (spayed 10). The most common breeds was domestic short hair (DSH) (n = 22), mixed breed (n = 4), Scottish fold (n = 2) and other breeds (n = 1 each) including Persian and American short hair. The mean ± SD of age was 44.33 ± 46.33 months or 3.60 ± 3.80 years. The mean ± SD of body weight was 3.45 ± 1.13 kg. The minimal body condition score was 2 and the maximal body condition score was 5 of 5. The mean ± SD of body condition score was 3.16 ± 0.83 and mode of body condition score was 3.

The clinical features of the 10 normal cats in group 1 that the age up to 7 months old are shown in Table 6. There were 5 males and 5 females (spayed 1). DSH was the most common breeds (n = 10). The mean ± SD of age was 6.10 ± 1.28 months or 0.5 ± 0.1 years. The mean ± SD of body weight was 2.78 ± 0.80 kg. The minimal body condition score was 2 and the maximal body condition score was 3 of 5. The mean ± SD of body condition score was 2.60 ± 0.51 and mode of body condition score was 3.

The clinical features of the 10 normal cats in group 2 that the age ranged from 7 months old to 7 years olds are shown in Table 7. There were 4 males (castrated 3) and 6 females (spayed 2). The most common breeds were DSH and mixed breed (n = 4 each) and other breeds (n = 1 each) including Persian and American short hair. The mean ± SD of age was 21.40 ± 12.57 months or 1.7 ± 1.0 year. The mean ± SD of body weight was 3.33 ± 1.27 kg. The minimal body condition score was 2 and the maximal body condition score was 4 of 5. The mean ± SD of body condition score was 3.00 ± 0.81 and mode of body condition score was 3.

The clinical features of the 10 normal cats in group 3 that the age more than 7 years old are shown in Table 7. There were 3 males (castrated 3) and 7 females (spayed 7). The mean ± SD of age was 105.60 ± 19.43 months or 8.80 ± 1.60 years. The mean ± SD of body weight was 4.24 ± 0.82 kg. DSH was the most common breed (n = 8) and 2 Scottish fold. The minimal body condition score was 3 and the maximal body condition score was 5 of 5. The mean ± SD of body condition score was 3.90 ± 0.56 and mode of body condition score was 4.

Table 5 *Clinical demographic data of 30 healthy cats.*

Clinical features		Value
No. of patients		30
Age (months)		
	Median	18
	Mean ± SD	44.33 ± 46.33
	Range	(4 - 132)
Sex		
	Female	18
	Intact	8
	Spayed	10
	Male	12
	Intact	6
	Castrated	6
Weight (kg.)		
	Median	3.45
	Mean ± SD	3.45 ± 1.13
	Range	(1.5 - 5.7)
Body condition score (5)		
	Median	3
	Mean ± SD	3.16 ± 0.83
	Range	(2 - 5)
	Mode	3

Table 6 *Clinical demographic data of 10 cats in group 1.*

Clinical features		Value
No. of patients		10
Age (months)		
	Median	7
	Mean ± SD	6.10 ± 1.28
	Range	(4.0 - 7.0)
Sex		
	Female	5
	Intact	4
	Spayed	1
	Male	5
	Intact	5
	Castrated	0
Weight (kg.)		
	Median	2.78
	Mean ± SD	2.78 ± 0.80
	Range	(1.5 - 4.1)
Body condition score (5)		
	Median	5
	Mean ± SD	2.60 ± 0.51
	Range	(2 - 3)
	Mode	3

Table 7 *Clinical demographic data of 10 cats in group 2.*

Clinical features		Value
No. of patients		10
Age (months)		
	Median	18
	Mean ± SD	21.40 ± 12.57
	Range	(11.0 - 48.0)
Sex		
	Female	6
	Intact	4
	Spayed	2
	Male	4
	Intact	1
	Castrated	3
Weight (kg.)		
	Median	3.33
	Mean ± SD	3.33 ± 1.27
	Range	(1.5 - 5.0)
Body condition score (5)		
	Median	3
	Mean ± SD	3.00 ± 0.81
	Range	(2 - 4)
	Mode	3

Table 8 *Clinical demographic data of 10 cats in group 3.*

Clinical features			Value
No. of patients			10
Age (months)			
	Median		96
	Mean ± SD		105.60 ± 19.43
	Range		(84.0 - 132.0)
Sex			
	Female		7
		Intact	0
		Spayed	7
	Male		3
		Intact	0
		Castrated	3
Weight (kg.)			
	Median		4.24
	Mean ± SD		4.24 ± 0.82
	Range		(2.9 - 5.7)
Body condition score (5)			
	Median		4
	Mean ± SD		3.90 ± 0.56
	Range		(3 - 5)
	Mode		4

Summary of clinical features

1. Sex

Among 30 normal cats in this study, 12 male cats had the higher body weight (3.96 ± 1.04 kg) than that of 18 female cats (3.10 ± 1.09 kg) (Figure 22). In addition, the sterilization had the effect to the body weight by significantly increasing the body weight in the 16 sterilized cats (both of male and female; 4.10 ± 0.92 kg) than that of the 14 intact cats (both of male and female; 2.70 ± 0.87 kg; p = 0.002; Figure 23). The stronger statistical significance was detected in female cats (10 spayed female cats compared to 8 intact female cats; 3.85 ± 0.89 and 2.26 ± 0.63 kg, respectively; p = 0.002; Figure 24) than that of the male cats (6 castrated male cats compared to the 6 intact male cats; 4.65 ± 0.73 and 3.28 ± 0.85 kg, respectively; p = 0.006; Figure 25). Besides comparing between the 6 intact male and 8 intact female cats, the significantly higher body weight was detected in intact male cats (3.28 ± 0.85 kg for the intact male cats and 2.26 ± 0.63 kg for intact female cats; p = 0.02; Figure26).

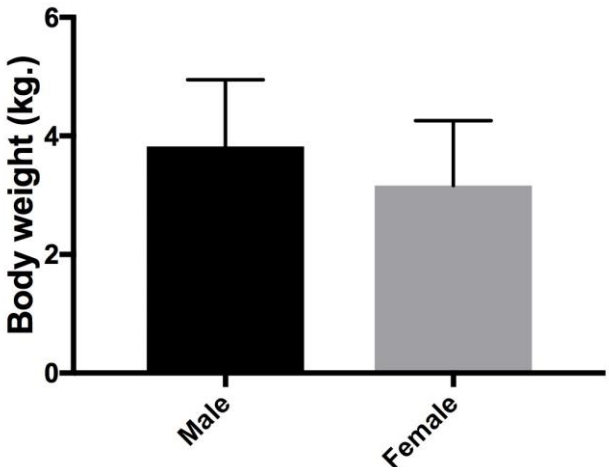

Figure 22 *The mean ± SD of body weight of male and female cats. From graph, male cats had more body weight than that of the female cats but significance did not be detected*

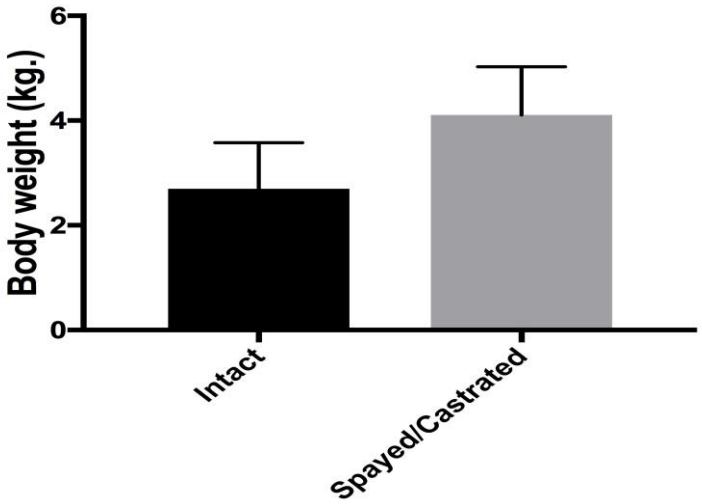

Figure 23 *The mean ± SD of body weight comparing between the intact male cats and sterilized cat, the intact cats had significantly lower body weight than that of the sterilized cats (p = 0.0002).*

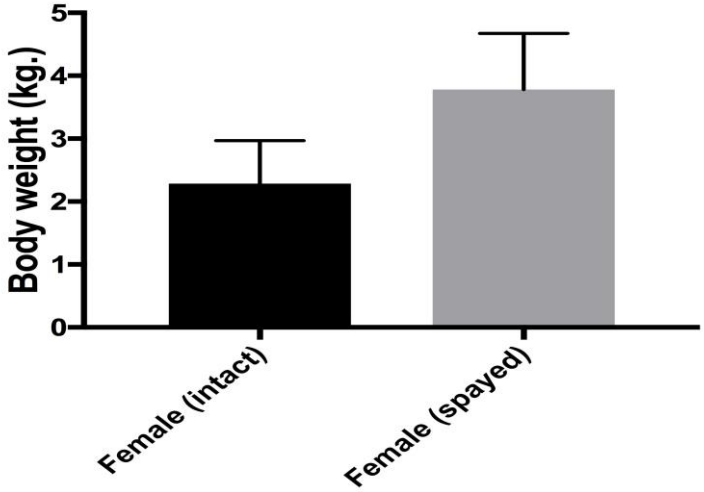

Figure 24 *The mean ± SD of body weight comparing between the intact female cats and spayed female cats, the intact female cats had significantly lower body weight than that of the spayed female cats (p = 0.002).*

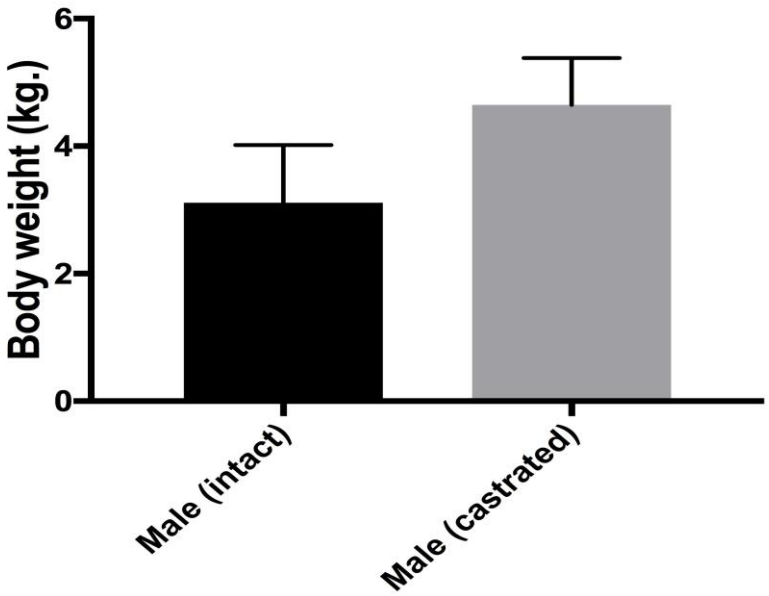

Figure 25 *The mean ± SD of body weight comparing between the intact male cats and castrated male cats, the intact male cats had significantly lower body weight than that of the castrated male cats (p = 0.006).*

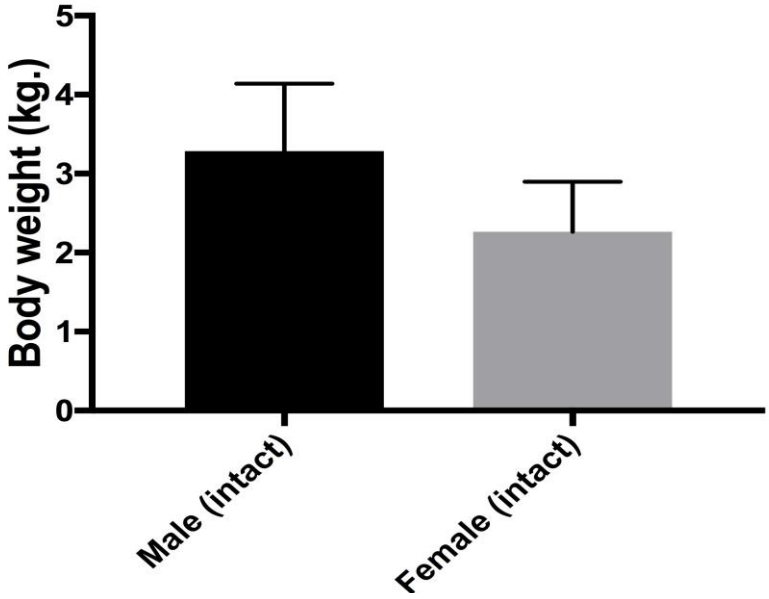

Figure 26 *The mean ± SD of body weight of intact male and intact female cats, the intact male cats had significantly higher body weight than that of the female cats* (*p* = 0.02).

2. Body condition score

Similar result of the body condition score from the thirty normal cats was detected by the fact of sterilization status. The sterilized cats had significant higher body condition score than that of the intact cats ($p < 0.0001$; Figure 27). The mean ± SD of body condition score of the intact cats and sterilized cats was 2.57 ± 0.51 and 3.68 ± 0.70, respectively. The mean ± SD of body condition score of the intact male cats was 2.83 ± 0.40 which was significantly lower than that of the castrated male cats (4.00 ± 0.63; $p = 0.003$; Figure 28) and the mean ± SD body condition score of intact female cats was 2.37 ± 0.51 which was significantly lower than that of the spayed female cats (3.50 ± 0.70; $p = 0.001$; Figure 29). Observed through the sex, the significant difference could not be detected (data did not show).

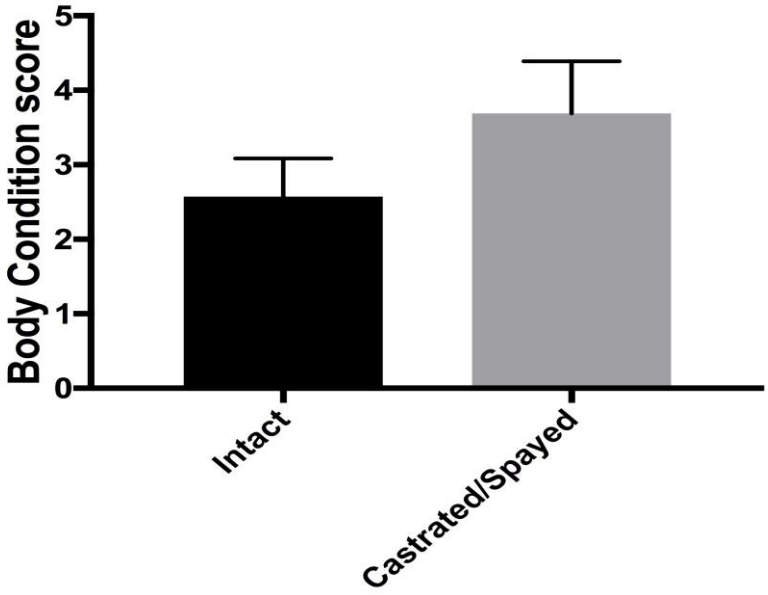

Figure 27 *The mean ± SD of body condition score the sterilized (castrated and spayed) cats was significantly higher than that of the intact cats (p < 0.0001).*

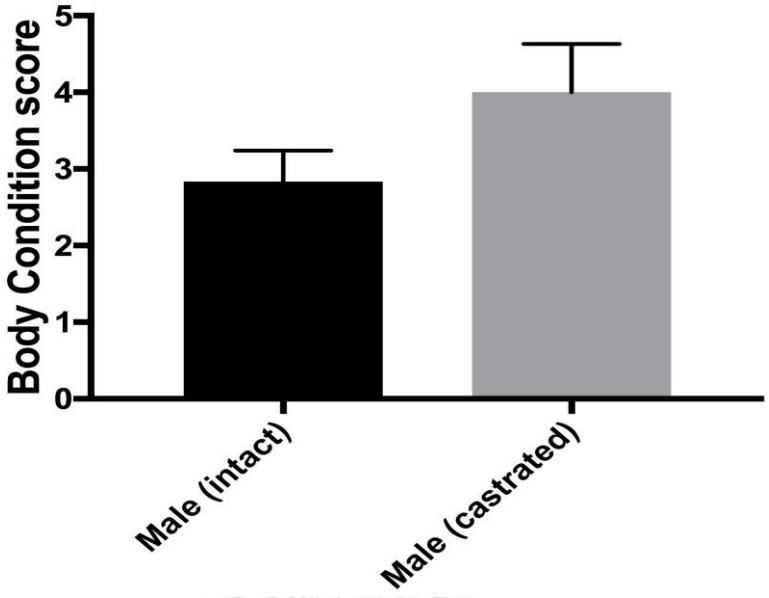

Figure 28 *The mean ± SD of body condition score of the castrated male cats was significantly higher than that of the intact male cats (p = 0.003).*

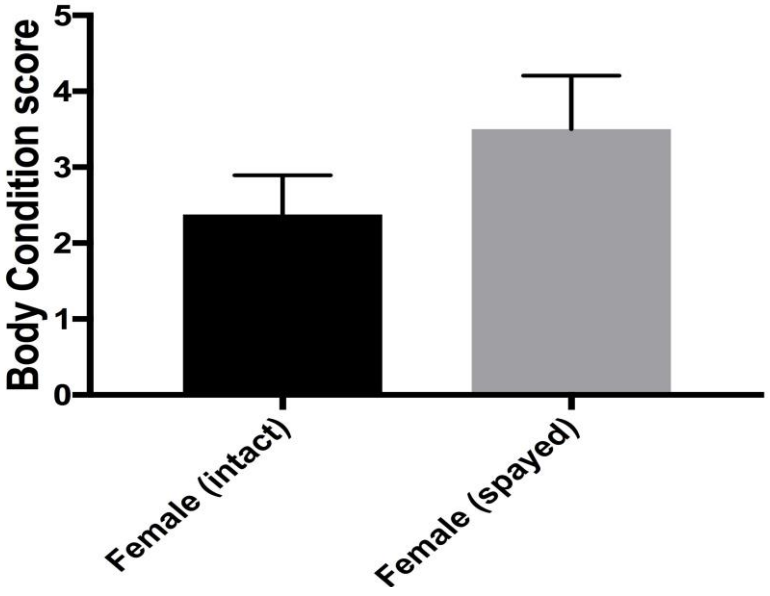

Figure 29 *The mean ± SD of body condition score of the spayed female cats was significantly higher than that of the intact female cats (p = 0.001).*

CT-based finding

1. The degree of obesity

The degree of obesity was measured on CT images and calculated as the ratio between the average lateral thoracic wall fat thickness at mid thoracic area (carina area) to the thoracic vertebral height on the same image. The mean ± SD of the degree of obesity of 30 normal cats, the cats in group1, the cats in group 2 and the cats in groups 3 were 0.08 ± 0.69, 0.54 ± 0.34, 0.58 ± 0.65 and 1.28 ± 0.97, respectively.

Table 9 *The mean ± SD of the degree of obesity.*

Group	Mean ± SD of the degree of obesity
All cats	0.80 ± 0.69
Group 1 (aged up to 7 months)	0.54 ± 0.34
Group 2 (aged 7 months to 7 years)	0.58 ± 0.65
Group 3 (aged more than 7 years)	1.28 ± 0.79

Summary of degree of obesity

Observing through the sex, the degree of obesity was higher in male cats compared to that of the female cats. Besides, the sterilization showed similar result as the body weight that sterilized cats had the higher degree of the obesity than that of the intact cats, the statistical significance could not be detected though.

Nevertheless, age, body weight and body condition score revealed statistically correlated to the degree of obesity as the following data. The correlation between age and the degree of obesity was R^2 = 0.2282; *p* = 0.007; Figure 30). The correlation between body weight and body condition score was R^2 = 0.4064; *p* = 0.0002; Figure 31). The correlation between body condition score and the degree of obesity was R^2 = 0.4752; *p* <0.0001; Figure 32).

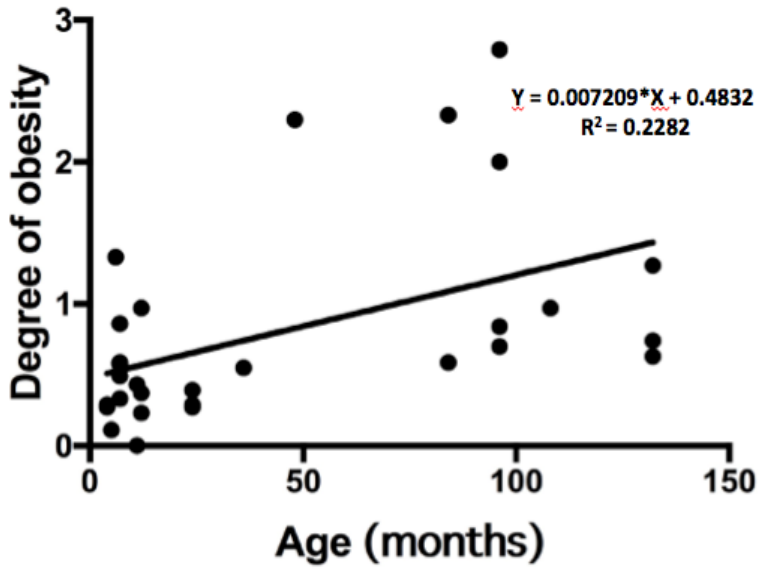

Figure 30 *Correlation between age and the degree of obesity among 30 cats* (*p* = 0.007).

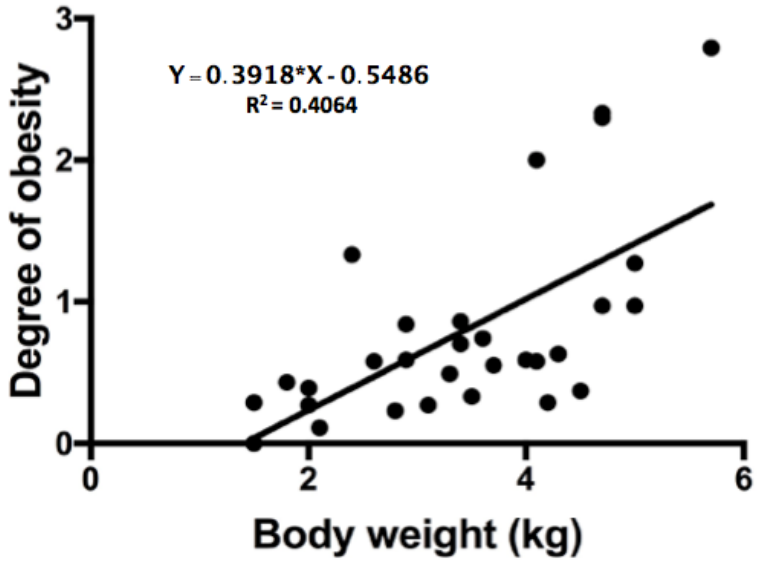

Figure 31 *Correlation between the body weight and the degree of obesity among 30 cats (p = 0.0002).*

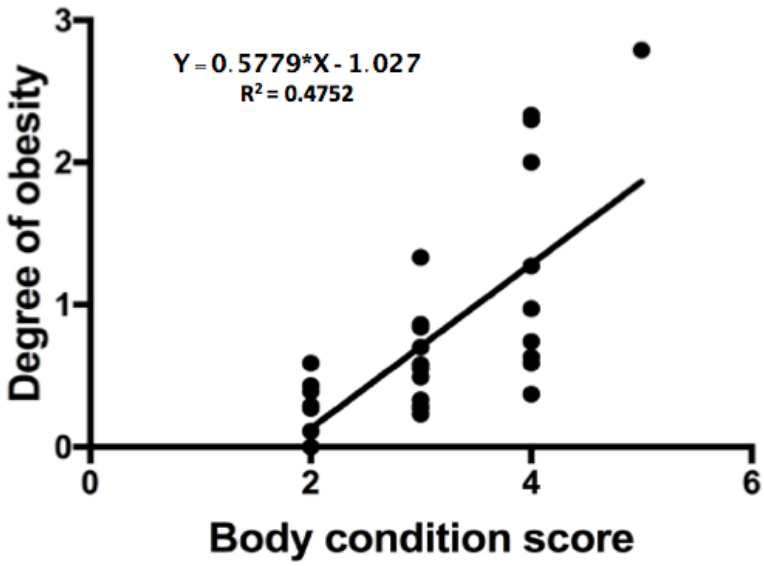

Figure 32 *Correlation between body condition score and the degree of obesity among 30 cats (p < 0.0001).*

2. Intra-thoracic lymph nodes

Among 4 locations of intra thoracic lymph nodes, only 3 of sternal, cranial mediastinal and tracheobronchial lymph nodes could be prominently detected on the contrast enhanced CT images. The shape of all lymph nodes was ellipse with homogeneous, enhanced soft tissue parenchyma. Sternal lymph node was detected in 6 of 30 cats. It embedded in fat above the second sternebra (Figure 33). The average size of sternal lymph node was 3.93 x 8.38 x 3.84 mm (W x L x H). The mean ± SD of volume of sternal lymph node was 54.05 ± 50.43 mm^3 and the mean ± SD of the widest of sternal lymph node on axial plane was 4.18 ± 1.62 mm. Cranial mediastinal lymph node was detected in 10 of 30 cats. They were found at least 2 positions that scattered into the cranial mediastinal fat next to the large blood vessels (Figure 34). The average size of cranial mediastinal lymph node was 4.67 x 7.42 x 3.40 mm (W x L x H). The mean ± SD of volume of cranial mediastinal lymph node was 60.30 ± 60.50 mm^3 and the mean ± SD of the widest of cranial mediastinal lymph node on axial plane axial plan was 5.07 ± 2.41 mm. Tracheobronchial lymph node was detected in 7 of 30 cats. They were found at least 4 positions that scattered at the termination of trachea and principle bronchi (Figure 35). The average size of tracheobronchial lymph node was 3.51 x 4.86 x 2.95 mm (W x L x H). The mean ± SD of volume of tracheobronchial lymph node was 55.84 ± 101.95 mm^3 and the widest of tracheobronchial lymph node on axial plane was 4.30 ± 2.19 mm (Table 10).

Group 1

Among 10 cats, there was only one location of intra-thoracic lymph node in one cat (1/10) that was the cranial mediastinal lymph node was detected on the post-contrasted enhanced CT images. The shape of lymph nodes was ellipse shape with homogeneous enhanced soft tissue appearance. Cranial mediastinal lymph node was embedded in the cranial mediastinal fat, next to the large blood vessels. The size of

cranial mediastinal lymph node was 5.90 x 9.59 x 3.08 mm (W x L x H). The volume of cranial mediastinal lymph node was 90.27 mm^3 and the widest of cranial mediastinal lymph node on axial plane was 5.90 mm (Table 11). In addition, a large, irregular shape, soft tissue structure located at the cranial mediastinal area was detected. This structure was suspected to be the thymus (Figure 36).

Group 2

There were 3 locations of intra-thoracic lymph nodes that were sternal, cranial mediastinal and tracheobronchial lymph nodes that were detected on the post-contrasted enhanced CT images. The shape of all lymph nodes was ellipse shape with homogeneous enhanced soft tissue appearance. Sternal lymph node was detected in 3 of 10 cats. It embedded in the fat above the second sternebra. The average size of sternal lymph node was 4.46 x 9.75 x 4.60 mm (W x L x H). The mean ± SD of volume of sternal lymph node was 76.27 ± 60.83 mm^3 and the mean ± SD of most the widest of sternal lymph nodes on the axial plane was 4.75 ± 2.03 mm. Cranial mediastinal lymph nodes were detected in 2 of 10 cats. They were found at least 2 positions that scattered in the cranial mediastinal fat next to the large blood vessels. The average size of cranial mediastinal lymph node was 3.28 x 6.52 x 3.14 mm (W x L x H). The mean ± SD of volume of cranial mediastinal lymph node was 34.01 ± 43.68 mm^3 and the mean ± SD of the most the widest of cranial mediastinal lymph node on the axial plane was 4.09 ± 0.98 mm. Tracheobronchial lymph node was detected in 2 of 10 cats. It was scattered at the termination of trachea and principle bronchi. The average size of tracheobronchial lymph node was 2.67 x 2.92 x 2.36 mm (W x L x H). The mean ± SD of volume of tracheobronchial lymph node was 6.46 ± 3.88 mm^3 and the mean ± SD of the widest of tracheobronchial lymph node on axial plane was 2.67 ± 0.32 mm (Table 12).

Group 3

There were 3 locations of intra-thoracic lymph nodes which were sternal, cranial mediastinal and tracheobronchial lymph nodes that were detected. On the post-contrasted enhanced-CT images, the shape of all lymph nodes was ellipse shape. Sternal lymph node was detected in 3 of 10 cats. It embedded in fat above the second sternebra. The average size of sternal lymph node was 3.41 x 7.02 x 3.09 mm (W x L x H). The average volume of sternal lymph node was 31.84 ± 34.31 mm^3 and the widest of sternal lymph node on axial plane was 3.60 ± 1.21 mm. Cranial mediastinal lymph node was detected in 7 of 10 cats. They were found at least 2 positions that scattered in the cranial mediastinal fat next to the large blood vessels. The average size of cranial mediastinal lymph node was 4.85 x 6.17 x 3.98 mm (W x L x H). The mean ± SD of volume of cranial mediastinal lymph node was 63.54 ± 69.14 mm^3 and the mean ± SD of the widest of cranial mediastinal lymph node on the axial plane was 5.24 ± 2.84 mm. Tracheobronchial lymph node was detected in 5 of 10 cats. They were found at least 4 positions that scattered to the termination of trachea and principle bronchi. The average size of tracheobronchial lymph node was 4.36 x 6.81 x 3.54 mm (W x L x H). The mean ± SD of volume of tracheobronchial lymph node was 75.61± 117.80 mm^3 and the widest of tracheobronchial lymph node on the axial plane was 4.95 ± 2.30 mm (Table 13).

Intercostal lymph node (Figure 37) was not detected on both of pre- and post-contrast CT images in all 30 normal cats.

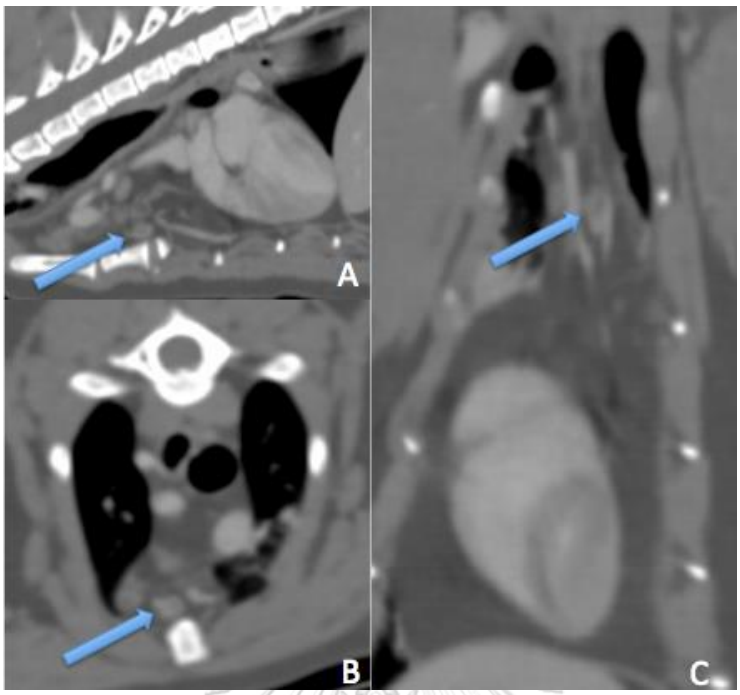

Figure 33 *Thoracic CT images of sternal lymph nodes (arrows) on each anatomical plane of sagittal (A), axial (B) and coronal (C) planes.*

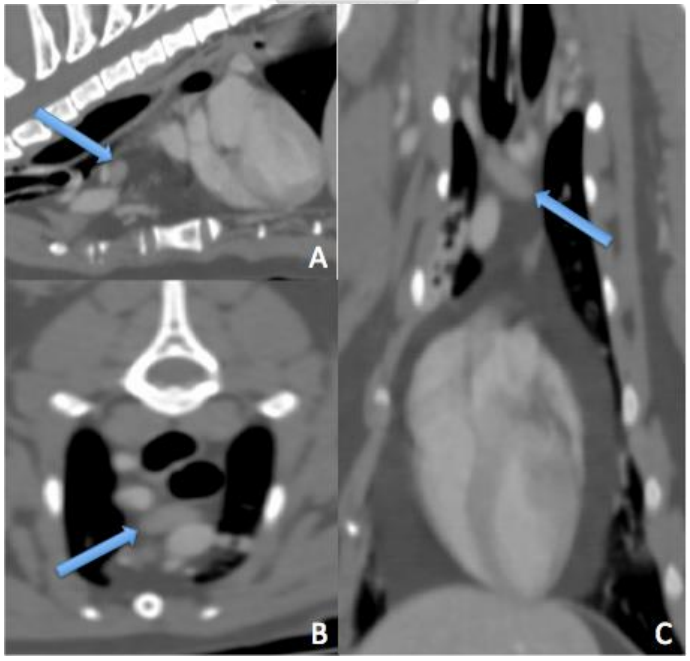

Figure 34 *Thoracic CT images of cranial mediastinal lymph nodes (arrows) on each anatomical plane of sagittal (A), axial (B) and coronal (C) planes.*

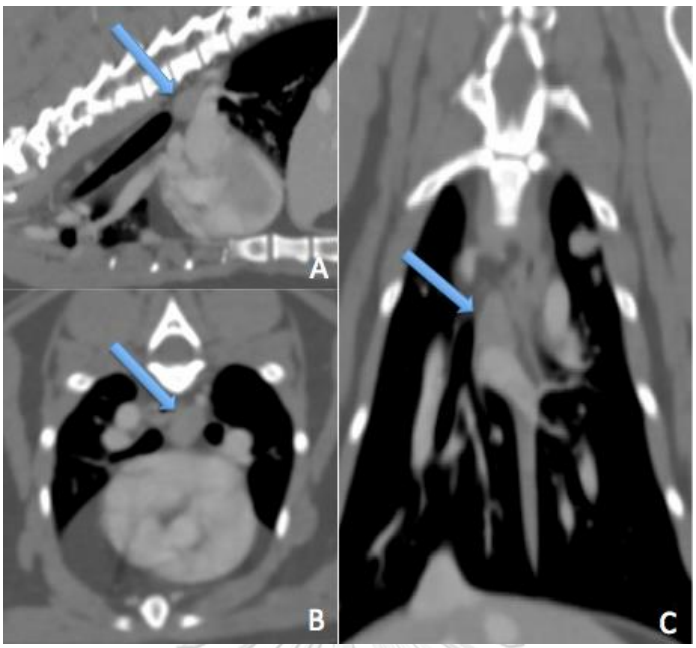

Figure 35 *Thoracic CT images of tracheobronchial lymph nodes (arrows) on each anatomical plane of sagittal (A), axial (B) and coronal (C) planes.*

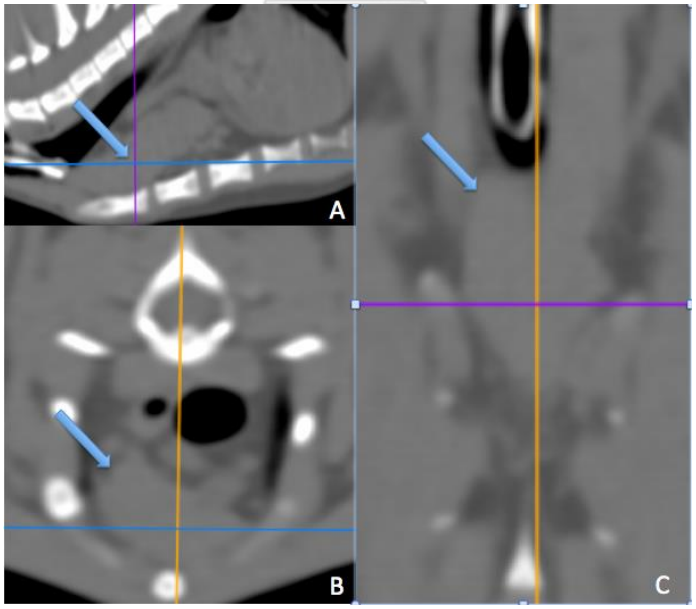

Figure 36 *Thoracic CT images of suspected area of thymus (arrows) on each anatomical plane of sagittal (A), axial (B) and coronal (C) planes.*

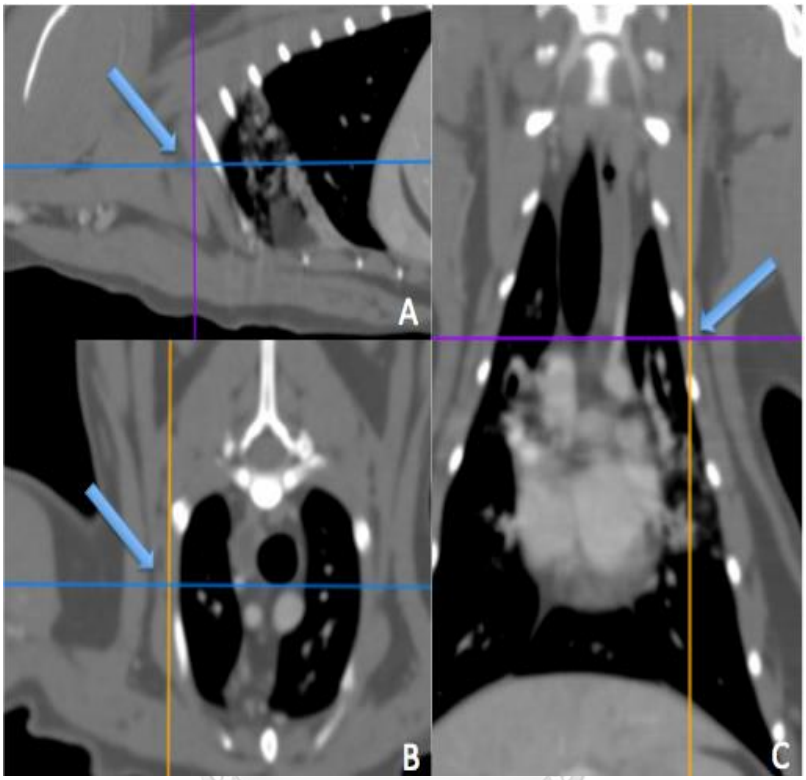

Figure 37 *Thoracic CT images of suspected area of intercostal lymph nodes (arrows) on each anatomical plane of sagittal (A), axial (B) and coronal (C) planes.*

Table 10 *Intra-thoracic lymph nodes 30 normal cats.*

Clinical features			Value
No. of patients			30
Location of lymph node			
Sternal lymph node			6
	Dimention	(mm)	3.93 x 8.38 x 3.84
	Volume	(mm^3)	54.05 ± 50.43
	the widest (axial plane)	(mm)	4.18 ± 1.62
Cranial mediastinum lymph node			10
	Dimention	(mm)	4.67 x 7.42 x 3.40
	Volume	(mm^3)	60.30 ± 60.55
	the widest (axial plane)	(mm)	5.70 ± 2.41
Tracheobronchial lymph node			7
	Dimention	(mm)	3.51 x 4.86 x 2.95
	Volume	(mm^3)	55.84 ± 101.95
	the widest (axial plane)	(mm)	4.30 ± 2.19

Table 11 *Intra-thoracic lymph nodes in group 1.*

Clinical features			Value
No. of patients			10
Location of lymph node			
Cranial mediastinum lymph node			1
	Dimention	(mm)	5.90 x 9.59 x 3.08
	Volume	(mm^3)	90.27
	the widest (axial plane)	(mm)	5.90

Table 12 *Intra-thoracic lymph nodes in group 2.*

Clinical features			Value
No. of patients			10
Location of lymph node			
Sternal lymph node			3
	Dimention	(mm)	4.46 x 9.75 x 4.60
	Volume	(mm^3)	76.27 ± 60.83
	the widest (axial plane)	(mm)	4.75 ± 2.03
Cranial mediastinum lymph node			2
	Dimention	(mm)	3.28 x 6.52 x 3.14
	Volume	(mm^3)	34.01 ± 43.68
	the widest (axial plane)	(mm)	4.09 ± 0.98
Tracheobronchial lymph node			2
	Dimention	(mm)	2.67 x 2.92 x 2.36
	Volume	(mm^3)	6.46 ± 3.88
	the widest (axial plane)	(mm)	2.67 ± 0.32

Table 13 *Intra-thoracic lymph nodes in group 3.*

Clinical features			Value
No. of patients			10
Location of lymph node			
Sternal lymph node			3
	Dimention	(mm)	3.41 x 7.02 x 3.09
	Volume	(mm^3)	31.84 ± 34.31
	the widest (axial plane)	(mm)	3.60 ± 1.21
Cranial mediastinum lymph node			7
	Dimention	(mm)	4.85 x 6.17 x 3.98
	Volume	(mm^3)	63.54 ± 69.14
	the widest (axial plane)	(mm)	5.24 ± 2.84
Tracheobronchial lymph node			5
	Dimention	(mm)	4.36 x 6.81 x 3.54
	Volume	(mm^3)	75.61 ± 117.80
	the widest (axial plane)	(mm)	4.95 ± 2.30

Factors of clinical demography that effect to the detection score of intra-thoracic lymph nodes.

In this study, age had effect to numbers of location of intra-thoracic lymph nodes that had detected in post-contrast enhanced CT images by intra-thoracic lymph nodes was detected only a node in a cat (1/10) in group 1 whereas 7 of nodes were detected in 6 cats (6/10) in group 2 and 15 of nodes were detected in 8 cats (8/10) in group 3, respectively. However, comparing between age, sex, body weight and body condition score had no effected to the detection score of intra-thoracic lymph nodes. Statistical significance between detection score and all factors was not found.

Factors of clinical demography that effect to volume and the widest on the axial plane of intra-thoracic lymph nodes.

1. Age

Age was not effect to the volume and the widest of lymph nodes. Statistical significance comparing between age and numbers of location of lymph nodes was not found.

2. Sex

Among 30 normal cats, male cats tended to have the higher volume of intra-thoracic lymph nodes than those of the female cats. However, statistical significance was not detected. In addition, sterilization was also not effect to the volume and the widest of the intra-thoracic lymph nodes.

3. Body weight

Body weight had no statistical significance to the volume, and the widest of intra-thoracic lymph node.

4. Body condition score

Body condition score had effect to the volume of intra-thoracic lymph nodes. The cats that had the body condition score 5/5 had significantly larger volume of intra-thoracic lymph nodes than those of other groups (p = 0.02; Figure 38). Nonetheless, body condition score had no effect on the widest of lymph node on the axial plane.

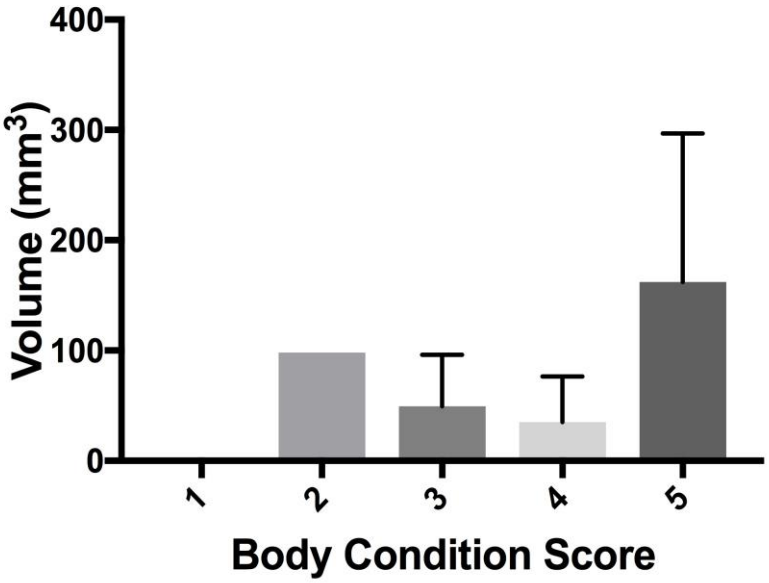

Figure 38 *The mean ± SD of the volume of lymph node was significantly higher in group 5 of body condition score (p = 0.02).*

Slice thickness.

Slice thickness was the parameter of CT machine that effected on the feasibility to identify of intra-thoracic lymph nodes in normal cats. From this study, slice thickness at different level such as 0.625, 1.25, 2.5, and 5 mm of post-contrast enhanced-CT had effected on the feasibility to identify the intra-thoracic lymph nodes in each area. Slice thickness at 0.625 mm had the highest detection score of the intra-thoracic lymph node, following by the 1.5, 2.5 and 5 mm, respectively. Statistical significance comparing between slice thickness at 0.625 mm and detection score was revealed ($p < 0.001$) (figure 39). Statistical significance of multiple comparisons between slice thickness at 0.625 mm and 1.25 mm was not found. However, statistical significance of multiple comparisons between slice thickness at 0.625 mm and 2.5 or 5.0 mm was showed ($p < 0.0001$) similar to the statistical significance result between slice thickness at 1.25 mm and 2.5 mm or 5mm ($p < 0.0001$).

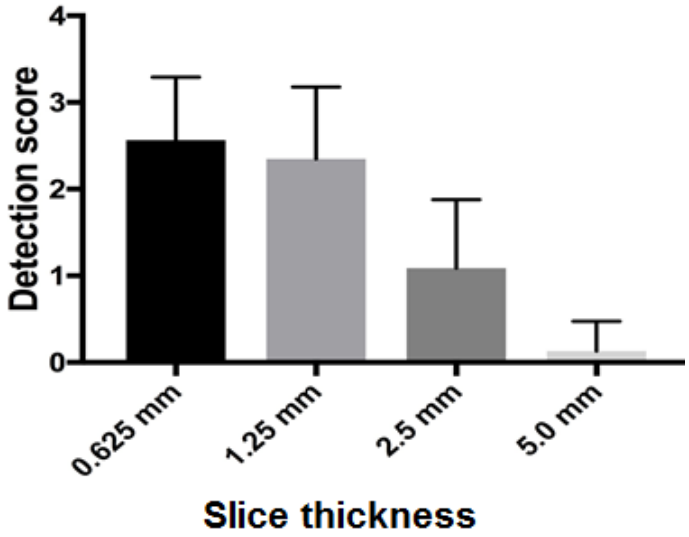

Figure 39 *The detection score of intra-thoracic lymph nodes at each slice thickness setting.*

Part 3: The CT appearance of intra-thoracic lymph node in feline patients.

CT data of feline patient that has been performed the CT scan as the diagnostic method at The Diagnostic Imaging Unit, The Small Animal Teaching Hospital, Faculty of Veterinary Science, Chulalongkorn University during May 2013 to March 2017 were retrieved. Since 2013, the data showed 654 patients which has been performed the CT scans, among those patients, there were 35 feline patients and they 18 feline patients were included in criteria. However, 9 of 18 feline patients had uncompleted post-contrast enhanced CT images due to incoherent between time and clearance of contrast enhancement thus data were not determined.

The clinical features of the 9 feline patients are shown in Table 14. There were 3 males (castrated 2) and 6 females (spayed 2). The most common breeds was domestic short hair (DSH) (n = 8) and a Persian cat. The mean ± SD of age was 96.00 ± 36.49 months or 8.00 ± 3.04 years. The mean ± SD of body weight was 4.44 ± 1.16 kg. The mean ± SD of degree of obesity based on CT images was 1.04 ± 1.44. The minimal degree of obesity was 0.00 and the maximal degree of obesity was 4.45. 6 of 9 cats were in obesity group 1, 2 of 9 cats were in obesity group 2 and only one cat was in obesity group 3. 8 of 18 feline patients were not found intra-thoracic lymph nodes. Only 1 of 18 patients was found cranial mediastinum mass (Figure 40) with pneumothorax.

Table 14 *Clinical demographic data of 9 feline patients.*

Clinical features		Value
No. of patients		9
Age (months)		
	Median	108.00
	Mean ± SD	96.00 ± 36.49
	Range	(48 - 144)
Sex		
	Female	6
	Intact	4
	Spayed	2
	Male	3
	Intact	1
	Castrated	2
Weight (kg.)		
	Median	4.00
	Mean ± SD	4.44 ± 1.16
	Range	(3.1 – 6.5)
Degree of obesity		
	Median	1.00
	Mean ± SD	1.04 ± 1.44
	Range	(0.00 – 4.45)

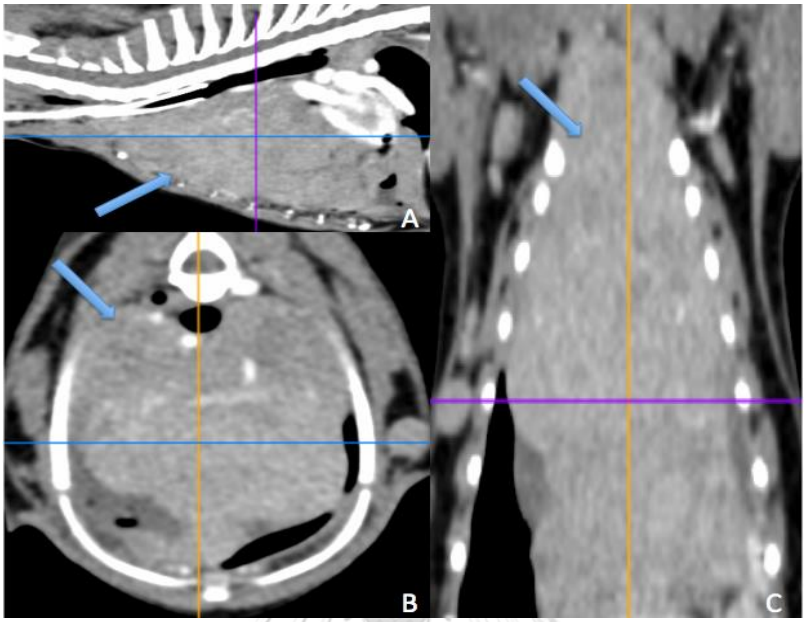

Figure 40 *Thoracic CT images of suspected cranial mediastinum mass in feline patient (arrows) on each anatomical plane of sagittal (A), axial (B) and coronal (C) planes.*

CHAPTER 5

DISCUSSION AND CONCLUSION

Lymphadenopathy is a pathological immune process responds by increased in size, change in shape or consistency of lymph nodes for protects body from antigen foreign body. Moreover, lymphadenopathy has been expressed by abnormal and unclear of margins, loss of the perinodal fat, heterogeneous of parenchyma and loss of hilus on advanced imaging (Nemanic et al., 2015). In cats, there had several diseases that cause lymphadenopathy both of infectious disease such as viral infection i.e. Feline leukemia virus, Feline immunodeficiency virus (Magden et al., 2011) and Feline peritonitis virus (Kipar et al., 2001), bacterial infection i.e. Hemoplasmosis and Mycoplasmosis (Little, 2012) and fungal infection like Crytococcosis and non-infectious disease including immune mediated, idiopathic, inflammation, foreign body (Vansteenkiste et al., 2014), neoplasia i.e. lymphoma (Louwerens et al., 2005; Seo et al., 2006), myeloma and mast cell tumor and non-neoplasia (Little, 2012).

The diagnostic evaluation of lymph nodes in cats is generally performed by physical examination. However, only the superficial lymph nodes could be successfully achieved. Other techniques that could be applied and provide more information of lymph nodes are survey radiograph, lymphangiography, ultrasonography, including cytologic or histologic examinations through fine needle aspiration or tissue biopsy (Rogers et al., 1993). CT scan had an advantage that eliminate the radiographic limitation by superimposition of anatomical structure such as thorax, head and neck area due to CT scan use computer for interpretation images that taken from many x-ray measurements from difference angels to create cross section images which allowing user to see inside the body without cutting (Ohlerth and Scharf, 2007; Bertolini

and Prokop, 2011). Accordingly, CT scan is the imaging method that non-invasive and could reveled deep anatomical structure as in the thorax better than other methods. Therefore, it is useful for diagnostic in cats (Dennler et al., 2013; Nemanic et al., 2015; Lacava et al., 2016).

The purpose of this study was to investigate the gross anatomy and computed tomographic appearance of intra-thoracic lymph nodes in feline soft cadavers, evaluated the appearance of normal intra-thoracic lymph nodes at each area both of before and after contrast enhanced-CT scan, evaluate the factor such as sex, age, body weight and body condition score of the cat effected to appearance of normal intra-thoracic lymph nodes and evaluated the parameter of CT machine such as slice thickness on the feasibility to detect the location of intra-thoracic lymph nodes at each area both of before and after contrast enhanced-CT scan.

Part 1: The gross appearance and computed tomographic appearance of intra-thoracic lymph nodes in presumed normal thorax of feline soft tissue cadavers.

From this study, the result showed that all intra-thoracic lymph nodes of 3 feline soft cadavers on pre-contrast enhance CT images were not detected due to disability to separating the anatomical structures in the feline thorax especially between intra-thoracic lymph nodes and surround soft tissue structure. Normally, for CT images of soft tissue structure, intravenous contrast agents are commonly applied for improvement the quality of CT images by act as opacifying agents to fulfill blood vessels, increasing the CT attenuation, confirming perfusion and promoting the image contrast between lesions and normal structure (Webb et al., 2015). Therefore, we recommended of using contrast medium for further investigating the feline thorax by

CT scan and comparing between pre- and post-contrast enhanced-CT images in order to accurate diagnosis.

Furthermore, using of feline soft tissue cadavers in this study, intra-thoracic lymph nodes could not be detected in all cats due to the putrefy of soft cadavers. It is suggested that using of fresh cadavers of animal for further studies would discover more interesting result.

Part 2: The CT appearance of intra-thoracic lymph node in normal cats.

30 normal cats of this study showed that male cats had the body weight higher than female cats and sterilized cats had the body weight higher than intact cats, both of male and female. Likewise, the body condition score and degree of obesity of male cats had higher than that of female cats and the sterilized cats had significant higher body condition score and degree of obesity than that of the intact cats. This result is alike the previous information that mean body weight of female cats was lower than male, and intact cats both of male and female have the percentage of overweight (BCS > 5) lower than sterilized cats (Kienzle and Moik, 2011). There had reported that sterilized cats had the body weight more than intact cats (McKenzie, 2010) due to hormone variations and increased food intake (Kanchuk et al., 2002; Wei et al., 2014).

The location of lymph nodes, which found in 30 normal cats, had 3 locations i.e. sternal, cranial mediastinal, and tracheobronchial lymph nodes. Interestingly, intercostal lymph node that located at under the pleura at the dorsal end of fifth or sixth intercostal space and drains of lymph at the structure of dorsal thoracic wall and send its efferent vessels to the cranial mediastinal nodes could not be detected.

Cranial mediastinal lymph nodes had found in all groups of ages. The average size of cranial mediastinal lymph node was 4.67 x 7.42 x 3.40 mm (W x L x H) and the mean ± SD of the widest of cranial mediastinal lymph node on axial plane was 5.07 ±

2.41 mm. Sternal and tracheobronchial lymph nodes had found in 2 groups of age (group 2 and 3). The average size were 3.93 x 8.38 x 3.84 and 3.51 x 4.86 x 2.95 mm (W x L x H) of sternal lymph nodes and tracheobronchial lymph nodes, respectively. The mean ± SD of the widest of sternal lymph node on axial plane was 4.18 ± 1.62 mm and 4.30 ± 2.19 mm for tracheobronchial lymph nodes. Nevertheless, the size of lymph node in post-contrast enhanced-CT images may be difference from soft tissue cadaver in part 1 which accurate measurement by caliper because the lymph nodes on CT images may not have been present in full thickness of craniocaudal direction similar to cadaver and dimension of lymph nodes in CT images was measuring based on transverse slices. Thus, dimension on CT images was overestimated as described in previous study (Beukers et al., 2013). Nonetheless, there had a report of quantitative assessment of the tracheobronchial lymph nodes and sternal lymph nodes at before including 41 and 81 days after inoculation with *Aelurostrongylus abstrusus* in 6 cats. The results showed the mean ± SD of dimension of intra-thoracic lymph nodes in the first day before inoculation was similar to our results. After infection at 48 and 81 days, thoracic radiographs including pre- and post- contrast enhanced-CT was perform. The result showed that intra-thoracic lymphadenopathy on radiography and pre- and post-contrast enhanced-CT images by increased attenuation with moderately lymphadenopathy which latter subsequently histopathological diagnosis as the reactive hyperplasia of the lymph nodes (Dennler et al., 2013).

Lacava and colleagues (2016) was reported that post-contrast enhanced-CT images were easily distinguishable the appearances of pulmonary and mediastinal lesions compared with thoracic radiographs in cats naturally infected with *A abstrusus*. Despite some reports, there had not much information of the detection, normal dimension and the widest of all intra-thoracic lymph nodes in cats on the axial CT images.

Contrary to previous reports, size of intra-thoracic lymph nodes in juvenile cats that the lymph node could be detected on post-contrast enhanced CT image was not larger than adult cats (Nemanic and Nelson, 2012). Besides, juvenile cats in this study (age between 4 months old to 12 months old) had been found a large, irregular shape, soft tissue structure located at the cranial mediastinal area that structure was suspected to be thymus. In dog, there had been reported that thymus was not disappearing but they were progressive involution during period from 6 to 23 months of age (Ploemen et al., 2003). Radiographically, thymus would be disappeared by the 8 to 10 months of age (Thrall, 2013). In human medicine, thymus in youngest children was tended to be larger than that in the adult though all age the size of thymus were varied considerably (Heiberg et al., 1982; Nishino et al., 2006; Lucaya and Strife, 2008; Simanovsky et al., 2012). Simanovsky and colleagues (2012) indicated that volume and density of thymus in human was decreased progressively with age and older patient with age 54 years old was still seen thymus with no solid tissue component. Additionally, the size of normal thymus in human was reported to be 1.1 ± 0.4 cm from age 6-19 years and decreased to 0.5 ± 0.27 cm for patients over the age of 50 years (Nishino et al., 2006). To the author's knowledge, information about time of thymus to be decreased in size in cats has not been previously reported. Based on this study, the oldest cat that had been found soft tissue structure at cranial mediastinal area that suspected as thymus in post-contrast enhanced-CT images was 12 months. Nevertheless, we had not performed autopsy the juvenile feline cadavers that age less than 12 months for confirming from pre-contrast enhance-CT images. Further study comparing the CT images and autopsy would be elucidated more information of the thymus.

Body weight, body condition score and degree of fat were described as factors that affected to detection score of lymph nodes in a previous studied (Nemanic and Nelson, 2012; Beukers et al., 2013). In the present study, cats in group 3 had the most

of mean ± SD of body weight, body condition score and degree of fat. This could be effect to the efficacy to detect the intra-thoracic lymph node compared to the cats in group 1 and 2. Nonetheless, due to the less number of the cat in group 1 and 2 that could be found the intra-thoracic lymph node, the statistical differences could not be detected.

Determining through the body condition score, the cat with body condition score 5 had lager volume of lymph node. This might be resulting from fat in the hilus of the lymph node that was an area which fat-attenuating structure entering a lymph node (Nemanic and Nelson, 2012). From previous study reported that hilus is present for blood and lymph use to enter and exist in normal lymph nodes. Loss of the hilus on diagnostics imaging has been associated about neoplastic infiltration in multiple species (Nyman and O'Brien, 2007; Nemanic et al., 2015). To the author's knowledge, the relationship between hilus of lymph node and volume of the lymph node has not been previously reported. Therefore, it is assumed that the larger body condition score with higher the degree of obesity might effect to the hilar fat deposition, which subsequently effect to the volume of the lymph node.

Slice thickness is one of factor that effect to image quality of CT images (Yu et al., 2009; Solomon et al., 2013). Yu and colleagues (2009) reported that the scan range should be considered as small as possible due to relate total radiation dose delivered to patient. In addition to the area, slice thickness at difference level such as 0.625, 1.25, 2.5 and 5 mm effect on the feasibility to identify of intra-thoracic lymph nodes in each area. From present study, slice thickness at 0.625 mm had the highest detection score of the intra-thoracic lymph nodes. In human, they had reported about small size of children required slice thickness in CT scan thinner than adult but in the similarly level of mAs, thinner slice increased noise compared with thicker slice. (Khong et al., 2012). In dogs, Ballegeer et al (2010) recommended slice interval for CT examination of the tracheobeonchial lymph nodes was 1.0-1.5 mm similar to present study,

statistical significance between slice thickness at 0.625 mm and 1.25 mm in this study was not found. Therefore, slice thickness at 1.25 mm is appropriates for applied in CT scan for detected intra-thoracic lymph nodes due to reduction of radiation risk for animal, providing of better signal noise ratio and good for data management in the server.

Part 3: The CT appearance of intra-thoracic lymph node in feline patients.

9 cats from feline patients that have been performed the CT scan as the diagnostic method at The Diagnostic Imaging Unit, The Small Animal Teaching Hospital, Faculty of Veterinary Science, Chulalongkorn University during May 2013 to March 2017 included criteria. 8 of 9 cats had not found intra-thoracic lymph nodes. In addition to the incoherent between time of injection and clearance of contrast medium, obesity score of most cats was lower in degree. This might be due to the affected disease induced the chronic cachexia and weight loss. Therefore, less intra-thoracic fat deposition that surrounding and enhancing the detection of small intra-thoracic lymph nodes would be a major factor of inability of detection in 8/9 cats. However, only 1 data had identified lymphadenopathy by CT images. The limitation of this patient was the complete for definite diagnosis for intra-thoracic mass that it was limitation of retrospective data. However, the history taking and physical examination showed feline leukemia virus infection, which this feline patient infected before detected intra-thoracic lymphadenopathy. From previous study, they had reported about infection of retro virus in cat have been associated with feline lymphoma (Beatty et al., 1998; Hartmann, 2011; Magden et al., 2011; Beatty, 2014; Fabrizio et al., 2014). However Seo and colleagues (2006) reported case study that found mediastinal mass in 8-month-old cat that negative to feline leukemia virus and feline immunodeficiency test with final histopathology evaluation confirmed the mass to be a lymphoma. From previous study, not only retroviral infection induced lymphoma can cause cranial mediastinal

mass found on imaging techniques but also other causes such as sternal or cranial mediastinal lymphadenopathy, mediastinal abscess, thymus, mediastinal cyst, foreign body, generalized megaesophagus, or neoplasis such as thymoma and lymphoma (Thrall, 2013). In addition to reported by Henninger (2003) that use of computed tomography in the diseased feline thorax showed 5 cats with thoracic diseased that confirmed by cytology between CT scan procedure in 4 cats which cause by adenocarcinoma (1/4), bronchial adenocarcinoma (2/4) and pulmonary carcinoma (1/4). Nevertheless all lesions that provide from advanced imaging techniques should be confirm with histopathology for definitive diagnosis (Henninger, 2003; Johnson et al., 2004; Paoloni et al., 2006; Jones and Pollard, 2012; Smith and O'Brien, 2012; Dennler et al., 2013; Patterson and Marolf, 2014; Nemanic et al., 2015; Lacava et al., 2016).

Advantage of this study

The current study of computed tomographic appearance of intra-thoracic lymph nodes in normal cats has provided the useful and novel knowledge about appearance of intra-thoracic lymph nodes such as location, shape, size and architectural pattern, especially at the post-contrast enhanced CT images. In addition, all of the involving factors to the diagnostic procedure such as the animal signalment and CT machine settings were clarify. All of the results from this study could be applied for the clinical practice of diagnostic imaging technique for scanning procedure and the size of intra-thoracic lymph nodes which were approximately 5.0 mm based on the widest of the axial, post-contrast enhanced CT image These results could be applied as the reference value for the clinical diagnosis of the feline patient.

Limitation

Although the current study has performed to reveal the information of intra-thoracic lymph nodes from several models such as feline soft tissue cadaver, clinically normal feline patient and a retrospective study of feline patients from clinical practice, some limitations have been found. Firstly, according to a small number of feline soft cadavers which the age of the cat was the maturity, the different structures such as intra-thoracic lymph node and thymus could not be compared on gross anatomy. In addition, to use the soft cadaveric model, the putrefy of the cadaver interfered the detection of structure on the CT images, especially the small structure such as the lymph node. Secondly, despite the pre- and post-contrast enhanced CT image were study in the clinically normal feline patients, the gross appearance could not be detected due to the ethically issue. Without the gross appearance observation on the alive cats or fresh cadavers, the intra-thoracic lymph nodes in the immature cats was hard to determine due to the less fat accumulation and concealment with thymus. Lastly, the retrospective study in the clinical feline patient showed the inhomogeneous CT data due to the different phase of post-contrast enhanced CT image. Without the proper phase of contrast enhancement, the ability to detect the normal size of intra-thoracic lymph node could be interfered. Furthermore, most of the feline patients were the chronic sick cats, the poor body condition score with less fat accumulation will also effect to the ability to detect the normal location and size of the normal lymph nodes. The larger sample size of the clinical study on the abnormal patients comparing the appearance of the size, shape, and architextural pattern of the post-contrast enhanced CT images would be differentiated the type of lymphadenopathy.

Conclusion

According to the study, to differentiate the normal lymph node from the lymphadenopathy in the thoracic cavity of feline patients, the veterinarian radiologist must take few considerations. First, Veterinarian radiologist should set CT scanning parameters at least the 1.25 mm of the slice thickness. With this condition, the detection of normal lymph node revealed the similar level to the thinner slice thickness. Besides, at the 1.25 mm of slice thickness, the clearer CT image would be accomplished due to the more signal noise ratio compared to the 0.625 mm of the slice thickness. Second, the intra-thoracic lymph node would be easily to detected in the post-contrast enhanced CT images. In the immature cat, intra-thoracic lymph nodes may be concealed with the thymus. Among the nodes, the normal intercostal lymph node was hard to observe and the widest of other intra-thoracic lymph nodes on the axial plane of CT image should be within 5.0 mm approximately. In the case of increase in the widest of the nodes or the appearance of intercostal lymph node on the post-contrast enhanced CT image, lymphadenopathy could probably be suspected. Lastly, the detection of intra-thoracic lymph node would be probably more in the senile, sterilized cats due to the increased of body condition score and fat accumulation.

REFERENCES

Aspinall V and O'Reilly M 2004. Introduction to Veterinary Anatomy and Physiology. 1 ed. In: The blood vascular system. Butterworth-Heinemamm, Toronto.

Ballegeer EA, Adams WM, Dubielzig RR, Paoloni MC, Klauer JM and Keuler NS 2010. Computed Tomography Characteristics of Canine Tracheobronchial Lymph Node Metastasis. Vet Radiol Ultrasound. 51(4): 397-403.

Beatty J 2014. Viral causes of feline lymphoma: retroviruses and beyond. Vet J. 201(2): 174-180.

Beatty JA, Lawrence CE, Callanan JJ, Grant CK, Gault EA, Neli JC and Jarrett O 1998. Feline immunodeficiency virus (FIV)-associated lymphoma: a potential role for immune dysfunction in tumourigenesis. Vet Immunol Immunopathol. 65: 309-322.

Bertolini G and Prokop M 2011. Multidetector-row computed tomography: Technical basics and preliminary clinical applications in small animals. Vet J. 189(1): 15-26.

Beukers M, Grosso FV and Voorhout G 2013. Computed Tomographic Characteristics of Presumed Normal Canine Abdominal Lymph Nodes. Vet Radiol Ultrasound. 54(6): 610-617.

Dennler M, Bass DA, Gutierrez-Crespo B, Schnyder M, Guscetti F, Di Cesare A, Deplazes P, Kircher PR and Glaus TM 2013. Thoracic Computed Tomography, Angiographic Computed Tomography, and Pathology Findings in Six Cats Experimentally Infected Withaelurostrongylus Abstrusus. Vet Radiol Ultrasound. 54(5): 459-469.

Dyce KM, Sack WO and Wensing CJG 2010. Textbook of Veterinary Anatomy. 4 ed. In: The cadiovascular system. Elsevier, Missouri.

Ettinger SN 2003. Principle of treatment feline lymphoma. Clin Tech Small Anim Pract. 18(2): 98-102.

Fabrizio F, Calam AE, Dobson JM, Middleton SA, Murphy S, Taylor SS, Schwartz A and Stell AJ 2014. Feline mediastinal lymphoma: a retrospective study of

signalment, retroviral status, response to chemotherapy and prognostic indicators. J Feline Med Surg. 16(8): 637-644.

Hartmann K 2011. Clinical aspects of feline immunodeficiency and feline leukemia virus infection. Vet Immunol Immunopathol. 143(3-4): 190-201.

Heiberg E, Wolverson MK, Sundaram M and Nouri S 1982. Normal Thymus: CT Characteristics in Subjects Under Age 20. AJR. 138: 491-494.

Henninger W 2003. Use of computed tomography in the diseased feline thorax. J Small Anim Pract. . 44: 56-64.

Hugo TB and Heading KL 2015. Prolonged survival of a cat diagnosed with feline infectious peritonitis by immunohistochemistry. Can Vet J. 56(1): 53-58.

Johnson VS, Ramsey IK, Thompson H, Cave TA, Barr FJ, Rudorf H, Williams A and Sullivan M 2004. Thoracic high-resolution computed tomography in the diagnosis of metastatic carcinoma. J Small Anim Pract. 45(3): 134-143.

Jones BG and Pollard RE 2012. Relationship between radiographic evidence of tracheobronchial lymph node enlargement and definitive or presumptive diagnosis. Vet Radiol Ultrasound. 53(5): 486-491.

Kanchuk ML, Backus RC, Calvert CC, Morris JG and Rogers QR 2002. Neutering Induces Changes in Food Intake, Body Weight, Plasma Insulin and Leptin Concentrations in Normal and Lipoprotein Lipase–Deficient Male Cats. J Nutr. 132: 1730-1732.

Khong PL, Frush D and Ringertz H 2012. Radiological protection in paediatric computed tomography. Ann ICRP. 41(3-4): 170-178.

Kienzle E and Moik K 2011. A pilot study of the body weight of pure-bred client-owned adult cats. Br J Nutr. 106 113-115.

Kipar A, Kohler K, Leukert W and Reinacher M 2001. A comparison of lymphatic tissues from cats with spontaneous feline infectious peritonitis (FIP), cats with FIP virus infection but no FIP, and cats with no infection. J Comp Pathol. 125(2-3): 182-191.

Lacava G, Zini E, Marchesotti F, Domenech O, Romano F, Manzocchi S, Venco L and Auriemma E 2016. Computed tomography, radiology and echocardiography in

cats naturally infected with Aelurostrongylus abstrusus. J Feline Med Surg. 19(4): 446-453.

Little SE 2012. The Cat: Clinical Medicine and Management. 1 ed. In: Hematology and Immune-Related Disorders. Elsevier, Missouri.

Louwerens M, London CA, Pedersen NC and Lyons LA 2005. Feline Lymphoma in the Post—Feline Leukemia Virus Era. J Vet Intern Med. 19: 329-335.

Lucaya J and Strife JL 2008. Pediactic chest imaging. 2 ed. In: Imaging Evaluation of theThymus and hymic Disorders in Children. Springer, Germany.

Magden E, Quackenbush SL and VandeWoude S 2011. FIV associated neoplasms—A mini-review. Vet Immunol Immunopathol. 143(3-4): 227-234.

McKenzie B 2010. Evaluating the benefits and risks of neutering dogs and cats. CAB Reviews: Perspectives in Agriculture, Veterinary Science, Nutrition and Natural Resources. 5(45): 1-18.

Nemanic S, Hollars K, Nelson NC and Bobe G 2015. Combination of Computed Tomographic Imaging Characteristics of Medial Retropharyngeal Lymph Nodes and Nasal Passages Aids Discrimination between Rhinitis and Neoplasia in Cats. Vet Radiol Ultrasound. 56(6): 617-627.

Nemanic S and Nelson NC 2012. Ultrasonography and noncontrast computed tomography of medial retropharyngeal lymph nodes in healthy cats. Am J Vet Res. 73(9): 1377-1385.

Nishino M, Ashiku SK, Kocher ON, Thurer RL, Boiselle PM and Hatabu H 2006. The thymus: A Comprehensive Review. RadioGraphics. 26: 335-348.

Nyman HT and O'Brien RT 2007. The sonographic evaluation of lymph nodes. Clin Tech Small Anim Pract. 22(3): 128-137.

Ohlerth S and Scharf G 2007. Computed tomography in small animals – Basic principles and state of the art applications. Vet J. 173(2): 254-271.

Paoloni MC, Adams WM, Dubielzig RR, Kurzman I, Vail DM and Hardie RJ 2006. Comparison of results of computed tomography and radiography with histopathologic findings in tracheobronchial lymph nodes in dogs with primary lung tumors 14 cases (1999–2002). J Am Vet Med Assoc. 228(1): 1718-1722.

Patterson MM and Marolf AJ 2014. Sonographic Characteristics of Thymoma Compared With Mediastinal Lymphoma. J Am Vet Med Assoc. 50(6): 409-413.

Ploemen JP, Ravesloot WT and van Esch E 2003. The incidence of thymic B lymphoid follicles in healthy beagle dogs. Toxicol Pathol. 31(2): 214-219.

Rogers KS, Barton CL and Landis M 1993. Canine and Feline Lymph Nodes. Part II. Diagnostic Evaluation of Lymphadenopathy. The Compendium. 15(11): 1490-1502.

Seo K-W, Choi U-S, Bae B-K, Park M-S, Hwang C-Y, Kim D-Y and Youn H-Y 2006. Case Report : Mediastinal lymphoma in a yong Turkish Aggora cat. J Vet Sci. 7(2): 199-201.

Simanovsky N, Hiller N, Loubashevsky N and Rozovsky K 2012. Normal CT characteristics of the thymus in adults. Eur J Radiol. 81(11): 3581-3586.

Smith K and O'Brien R 2012. Radiographic Characterization of Enlarged Sternal Lymph Nodes in 71 Dogs and 13 Cats. J Am Vet Med Assoc. 48(3): 176-181.

Solomon JB, Li X and Samei E 2013. Relating noise to image quality indicators in CT examinations with tube current modulation. AJR Am J Roentgenol. 200(3): 592-600.

Thrall DE 2013. Textbook of Veterinary Diagnostic Radiology. 6 ed. In: Chapter 30. The Mediastinum. ELSEVIER, Missouri.

Vansteenkiste DP, Lee KCL and Lamb CR 2014. Computed tomographic findings in 44 dogs and 10 cats with grass seed foreign bodies. J Small Anim Pract. 55(11): 579-584.

Webb WR, Brant WE and Major NM 2015. Fundamentals of body CT. 4 ed. In: ELSEVIER, Philadelphia.

Wei A, Fascetti AJ, Kim K and Ramsey JJ 2014. Post-castration variations in weight gain in a cohort of young adult male cats. J Nutr Sci. 3(37): 1-4.

Yu L, Liu X, Leng S, Kofler JM, Ramirez-Giraldo JC, Qu M, Christner J, Fletcher JG and McCollough CH 2009. Radiation dose reduction in computed tomography: techniques and future perspective. Imaging Med. 1(1): 65-84.

APPENDIX

VITA

Miss Ninlawan Thammasiri was born on May 7th, 1988 in Lampang province, Thailand. She achieved her bachelor degree of Doctor of Veterinary Medicine (D.V.M) from the faculty of Veterinary Medicine, Khon Kaen University in academic year 2012. After graduation, she had spent her second year to sought for off-university experienced in private small animal hospital. In 2014, she had to join the first generation of veterinary internship training program at Chulalongkorn University Veterinary Teaching Hospital. After that, in 2015, she entered the Master's Degree program in Department of Veterinary Surgery, Chulalongkorn University. Her special interest is focus on Veterinary Imaging.